Functional Divergence of Multiple Duplicated *Foxl2* Homeologs and Alleles in a Recurrent Polyploid Fish

Rui-Hai Gan,[1,2] Yang Wang,[1,2] Zhi Li,[1,2] Zhao-Xi Yu,[3] Xi-Yin Li,[1,2] Jin-Feng Tong,[1,2] Zhong-Wei Wang,[1,2] Xiao-Juan Zhang,[1,2] Li Zhou,*[,1,2] and Jian-Fang Gui*[,1,2]

[1]State Key Laboratory of Freshwater Ecology and Biotechnology, Institute of Hydrobiology, The Innovation Academy of Seed Design, Chinese Academy of Sciences, Wuhan, China

[2]University of Chinese Academy of Sciences, Beijing, China

[3]Ningxia Fisheries Research Institute, Yinchuan, China

***Corresponding authors:** E-mails: jfgui@ihb.ac.cn; zhouli@ihb.ac.cn.

Associate editor: Aida Ouangraoua

Abstract

Evolutionary fates of duplicated genes have been widely investigated in many polyploid plants and animals, but research is scarce in recurrent polyploids. In this study, we focused on *foxl2*, a central player in ovary, and elaborated the functional divergence in gibel carp (*Carassius gibelio*), a recurrent auto-allo-hexaploid fish. First, we identified three divergent *foxl2* homeologs (*Cgfoxl2a-B*, *Cgfoxl2b-A*, and *Cgfoxl2b-B*), each of them possessing three highly conserved alleles and revealed their biased retention/loss. Then, their abundant sexual dimorphism and biased expression were uncovered in hypothalamic–pituitary–gonadal axis. Significantly, granulosa cells and three subpopulations of thecal cells were distinguished by cellular localization of CgFoxl2a** and Cg**Foxl2b**, and the functional roles and the involved process were traced in folliculogenesis. Finally, we successfully edited multiple *foxl2* homeologs and/or alleles by using CRISPR/Cas9. *Cgfoxl2a-B* deficiency led to ovary development arrest or complete sex reversal, whereas complete disruption of *Cgfoxl2b-A* and *Cgfoxl2b-B* resulted in the depletion of germ cells. Taken together, the detailed cellular localization and functional differences indicate that *Cgfoxl2a* and *Cgfoxl2b* have subfunctionalized and cooperated to regulate folliculogenesis and gonad differentiation, and *Cgfoxl2b* has evolved a new function in oogenesis. Therefore, the current study provides a typical case of homeolog/allele diversification, retention/loss, biased expression, and sub-/neofunctionalization in the evolution of duplicated genes driven by polyploidy and subsequent diploidization from the recurrent polyploid fish.**

Key words: **polyploid, gibel carp, gynogenesis, ovary development, *foxl2*.**

Article

Introduction

Genome polyploidy has been thought as an evolutionary driving force (Otto 2007; Gui and Zhou 2010; Soltis PS and Soltis DE 2016; Zhou and Gui 2017), and its significance and implications on trait innovation and ecological adaption have been supported from whole-genome sequencing and comparative genomic analyses (Van de Peer et al. 2009, 2017; Soltis et al. 2014; Soltis PS and Soltis DE 2016; Cheng et al. 2018). It might result in the complexity, variability, and diversity of organisms, especially leading to an increased short-term adaptive potential (Van de Peer et al. 2017) and a long-term evolvability (Cheng et al. 2018). Therefore, polyploidy is considered as a main driver of speciation nowadays and shapes almost every aspect of species evolution (Sessa 2019). All plants and most of extant vertebrates have evolved from polyploid ancestors. Two rounds (2R) of whole-genome duplication (WGD) were proposed to trigger the species explosion of vertebrates, and a teleost-specific third WGD (Ts3R) was believed to lead to dramatic rise and rapid radiation of teleosts (Amores et al. 1998; Meyer and Van de Peer 2005). The neopolyploid might firstly undergo a chaos of "genomic shock" (McClintock 1984; Ng et al. 2012), subsequently occur a series of complicated non-Mendelian changes to shape a novel genome, and finally evolve into a paleopolyploid or a new diploid (Comai 2005; Otto 2007; Soltis et al. 2014; Zhou and Gui 2017). These processes are usually referred to as diploidization, during which duplicated genes undergo homeolog or allele diversification, fractionation, sub- or neofunctionalization under relaxed purifying selection (Liu et al. 2009; Cheng et al. 2018). Although the fates of duplicated genes have been well documented in paleopolyploids, the research is scarce in recurrent polyploids with complex genomes.

In addition to the 3R of WGD shared by all teleosts, polyploidy happened repeatedly in some taxonomic fish orders (Leggatt and Iwama 2003; Taylor 2003; Van de Peer et al. 2003; Gui and Zhou 2010; Zhou and Gui 2017; Lu et al. 2021). For

example, a salmonid-specific fourth WGD (Ss4R) and an allopolyploidy event were shown to have occurred in the common ancestor of salmonids (Berthelot et al. 2014; Lien et al. 2016) or common carp (*Cyprinus carpio*) (Xu et al. 2014), respectively. Polyploid *Carassius* species complex, widely distributing across the Eurasian continent (Liu, Jiang, et al. 2017, Liu, Li, et al. 2017), include allo-tetraploid crucian carp (*C. auratus*) with 100 chromosomes and auto-allo-hexaploid gible carp (*C. gibelio*) with over 150 chromosomes (Zhou and Gui 2002; Zhu et al. 2006; Yu et al. 2021). Two extra rounds of polyploidy, including an early allotetraploidy (4R) and a late autotriploidy (5R), were estimated to have undergone during the evolution of gibel carp (Li, Zhang, et al. 2014). Interestingly, gibel carp is able to reproduce by unisexual gynogenesis (Gui and Zhou 2010; Liu et al. 2015; Zhang et al. 2015). Compared with other unisexual vertebrates (Neaves and Baumann 2011), 1.2–26.5% male individuals were found in gibel carp natural populations (Jiang et al. 2013; Li et al. 2018), which is determined by extra microchromosomes and is affected by rearing temperature (Li et al. 2016; Li and Gui 2018; Li et al. 2018). A few key genes, such as dsx- and mab-3-related transcription factor 1 (*Dmrt1*) (Li, Li, et al. 2014) and a novel *Setdm* (SET domain-containing male-specific gene) located on extra microchromosomes (Li et al. 2017), show predominant or specific expression in gibel carp testis, but it is unclear which might serve as the initiator or master for ovary development in the all-female gynogenetic fish.

Foxl2, belonging to Forkhead (FKH) box (Fox) protein subfamily FoxL, was identified as the earliest key marker of mammal ovarian differentiation (Cocquet et al. 2002; Schmidt et al. 2004; Kocer et al. 2008; Uhlenhaut et al. 2009). Its predominant expression in ovary has been confirmed in some bisexual fishes (Loffler et al. 2003; Nakamoto et al. 2006; Alam et al. 2008; Ijiri et al. 2008; Bertho et al. 2016; Bhat et al. 2016; Yang et al. 2017) and its pivotal roles in ovarian differentiation have been revealed in zebrafish (*Danio rerio*) (Yang et al. 2017), Nile tilapia (*Oreochromis niloticus*) (Zhang et al. 2017), and rainbow trout (*Oncorhynchus mykiss*) (Bertho et al. 2018). Although *foxl2* is a conserved transcription factor in metazoan, its evolution in teleosts is complicated (Bertho et al. 2016). Zebrafish has two *foxl2* paralogs (*foxl2a* and *foxl2b*) resulted from Ts3R. They sequentially and cooperatively regulate zebrafish ovary development and maintenance, and *foxl2b* plays a dominant role during the process (Yang et al. 2017). In rainbow trout, *foxl2a* was lost after Ts3R whereas *foxl2b* was further duplicated into two coorthologs (*foxl2b1* and *foxl2b2*) following Ss4R, which carried the salmonid master sex-determining gene SdY into the nucleus to prevent female differentiation (Bertho et al. 2018). Nile tilapia retained only one *foxl2* gene and XX *foxl2*$^{-/-}$ mutant occurred female-to-male sex reversal (Zhang et al. 2017). Here, we chose gibel carp and *foxl2*, a recurrent hexaploid and master gene in ovary development, as a unique model to reveal the evolutionary fates of duplicated genes. We first investigated the diversification, evolution, and biased expression of *foxl2* homeologs and alleles in auto-allo-hexaploid gibel carp. Then, we tried to knockout multiple *foxl2* homeologs and/or alleles by using CRISPR/Cas9. Finally, we compared the sex ratio, gonadal histological structure, and dynamic changes of gonadal development-related gene expression among these mutants with wild-types (WTs) during oogenesis.

Results

Diversification and Characterization of *foxl2* Homeologs and Alleles

A total of 12 *Cgfoxl2* transcripts were cloned from hexaploid gibel carp ovary by homology-based cloning strategy (supplementary fig. S1, Supplementary Material online) and mapped onto the assembled genome of gibel carp (fig. 1A). Multiple nucleotide alignments and phylogenetic analysis showed that six transcripts were annotated as *foxl2a* and others belonged to *foxl2b*. The six *Cgfoxl2b* transcripts were clustered into two groups (three *Cgfoxl2b-As* and three *Cgfoxl2b-Bs*) (fig. 1B). The average identities among three *Cgfoxl2b-As* or *Cgfoxl2b-Bs* were about $99.7 \pm 0.2\%$ and $99.3 \pm 0.1\%$ respectively, whereas the average identity between *Cgfoxl2b-As* and *Cgfoxl2b-Bs* was about $88.6 \pm 0.4\%$. These data suggest that *Cgfoxl2b-A* and *Cgfoxl2b-B* might be a pair of homeologs derived from early allotetraploidy (4R), and they both have three alleles because of late autotriploidy (5R). The major differences between *Cgfoxl2b-As* and *Cgfoxl2b-Bs* homeologs existed in the 5′ untranslated region (UTR) and the 3′ UTR. Thus, the transcripts of *Cgfoxl2b-As* and *Cgfoxl2b-Bs* were predicted to encode one *Cg*Foxl2b-A protein (*Cg*Foxl2b-A1/A2/A3) and two *Cg*Foxl2b-B proteins (*Cg*Foxl2b-B1/B2 and *Cg*Foxl2b-B3), and there was only one amino acid difference between *Cg*Foxl2b-B1/B2 and *Cg*Foxl2b-B3. *Cg*Foxl2b-A and *Cg*Foxl2b-B had about 95.0% amino acid identity (supplementary fig. S2, Supplementary Material online).

Unlike *Cgfoxl2b*, all six *Cgfoxl2a* transcripts were aligned to same position in the chromosome *Cg*B15 (fig. 1C). We could not find any other *Cgfoxl2a* gene in the assembled genome of gibel carp (Wang Y, Li XY, Wu B, Xu M, Wang ZW, Li Z, Zhang XJ, Yin Z, Yang YL, Miao LJ, et al., unpublished data) or clone any other *Cgfoxl2a* transcripts from ovary. Thus, these *Cgfoxl2a* transcripts were named as *Cgfoxl2a-B*, and *Cgfoxl2a-A* gene might be lost during evolution. According to the differences of 5′ UTR, *Cgfoxl2a-B* transcripts were also clustered into two classes (*Cgfoxl2a-B1/B2/B3-a* and *Cgfoxl2a-B1/B2/B3-b*), which came from the different transcriptional start sites at first and second exon of *Cgfoxl2a-B* genes, respectively (fig. 1A). Each of them also had three alleles, among which three and two single nucleotide polymorphism (SNP) existed in the open reading frame (ORF) and 3′ UTR, respectively. All *Cgfoxl2a-B* transcripts were predicted to encode the same *Cg*Foxl2a-B protein (*Cg*Foxl2a-B1/B2/B3).

*Cg*Foxl2a-B had 71.6% and 68.7% amino acid identities with *Cg*Foxl2b-A and *Cg*Foxl2b-B, respectively. As a comparative control, eight *Cafoxl2* transcripts were cloned from tetraploid crucian carp, which were predicted to encode two proteins of *Ca*Foxl2a-B, *Ca*Foxl2b-A, and *Ca*Foxl2b-B, respectively. We also could not find a region containing *foxl2a-A* in the assembled genome of crucian carp (Wang Y, Li XY, Wu B, Xu M, Wang ZW, Li Z, Zhang XJ, Yin Z, Yang YL, Miao LJ, et al., unpublished data) and gold fish (Luo et al. 2020) by using GMAP (Wu and

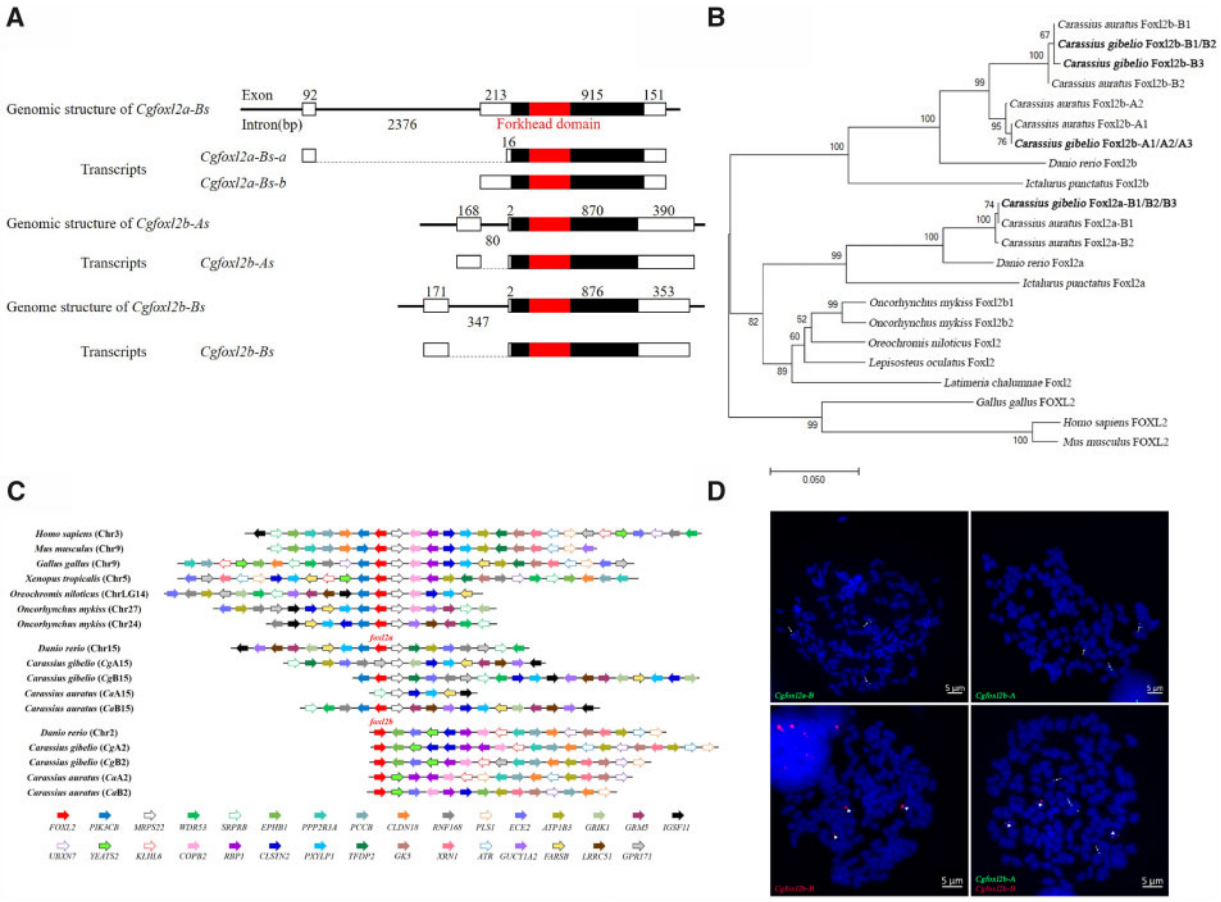

Fig. 1. Molecular characterization of gibel carp *foxl2a* and *foxl2b*. (*A*) Genomic structure and transcript sketch of *foxl2a* and *foxl2b*. Exons and introns are shown by rectangle boxes and thick lines, respectively, and their sizes (bp) are indicated upon or below. ORFs and FKH domain are highlighted by black and red boxes, respectively. (*B*) Phylogenetic tree of vertebrate Foxl2. (*C*) Gene synteny of vertebrate *foxl2*. Gibel carp *foxl2a-B*, *foxl2b-A*, and *foxl2b-B* are located on chromosome *Cg*B15, *Cg*A2, and *Cg*B2, respectively. Conserved gene blocks are represented in matching colors, and transcription orientations are indicated by arrows. (*D*) Localization on metaphase chromosomes of gibel carp *Cgfoxl2a-B*, *Cgfoxl2b-A*, and *Cgfoxl2b-B*. The chromosomes with green signals (indicated by arrows) were stained by *Cgfoxl2a-B*-BAC-DNA or *Cgfoxl2b-A*-BAC-DNA probe labeled with DIG, and the chromosomes with red signals (indicated by arrowheads) were stained by *Cgfoxl2b-B*-BAC-DNA probe labeled with Biotin. All metaphase chromosomes (blue) were counterstained with DAPI.

Watanabe 2005) or clone any of *Cgfoxl2a-A* transcripts, which suggested that *foxl2a-A* gene might have been lost in the ancestor of *Carassius* complex after 4R. Phylogenetic analysis showed that *Carassius* complex Foxl2a and Foxl2b were clustered with zebrafish and channel catfish (*Ictalurus punctatus*) Foxl2a and Foxl2b, respectively (fig. 1*B*). *Carassius* complex Foxl2b-A and Foxl2b-B were grouped into two independent branches, indicating *foxl2b-A* and *foxl2b-B* are duplicated in the ancestor of gibel carp and crucian carp. Rainbow trout Foxl2b1 and Foxl2b2, Nile tilapia Foxl2, spotted gar (*Lepisosteus oculatus*) Foxl2, and coelacanth (*Latimeria chalumnae*) Foxl2 were first grouped together and then clustered with other teleost Foxl2a. Finally, all fish Foxl2 clustered with tetrapod Foxl2.

Subsequently, the genomic structure and syntenic alignment were also analyzed (fig. 1*A* and *C*). All gibel carp *foxl2* genes have a biexonic structure same as zebrafish *foxl2* (Yang et al. 2017). *Cgfoxl2a-B*, *Cgfoxl2b-A*, and *Cgfoxl2b-B* are located on chromosome *Cg*B15, *Cg*A2, and *Cg*B2 of gibel carp, respectively (fig. 1*C*), and three alleles of each gene in the three homologous chromosomes were confirmed by fluorescent in situ hybridization (FISH) (fig. 1*D*). For example, three green *Cgfoxl2b-A* signals were observed from three homologous chromosomes, and three red *Cgfoxl2b-B* signals were located on another three homologous chromosomes when simultaneously using *Cgfoxl2b-A*-BAC-DNA and *Cgfoxl2b-B*-BAC-DNA as probes (fig. 1*D*). Our previous study had revealed a highly conserved synteny within genomic regions around vertebrate *foxl2* and a complementary loss/retention pattern of *foxl2a* and *foxl2b* vicinity genes between zebrafish chromosome 15 and chromosome 2 (Yang et al. 2017). Gibel carp chromosome *Cg*A15 and *Cg*B15 retained the overwhelming majority of genes located on zebrafish chromosome 15, except losing the conserved gene block (*pik3cb-foxl2*) in chromosome *Cg*A15. Compared with zebrafish chromosome 2, gibel carp chromosome *Cg*A2 and *Cg*B2 both retained most genes.

Divergent and Dynamic Expression Patterns in Brain–Pituitary–Gonad Axis

First, the distribution of *foxl2as* and *foxl2bs* mRNAs in adult tissues was analyzed by quantitative polymerase chain reaction

(qPCR). Due to the extremely high identities among three alleles of each *foxl2* gene (supplementary fig. S1, Supplementary Material online), four specific pairs of primers (supplementary table S1, Supplementary Material online) were designed to amplify *Cgfoxl2a-Bs-a*, *Cgfoxl2a-Bs-b*, *Cgfoxl2b-As*, and *Cgfoxl2b-Bs*, respectively. Compared with other analyzed tissues, abundant gibel carp *foxl2as* and *foxl2bs* transcripts were amplified from brain–pituitary–gonad axis (fig. 2*A*), indicating their important and conserved roles in reproductive regulation. In hypothalamus and other brains, *Cgfoxl2a-Bs-b* and *Cgfoxl2b-Bs* were both remarkably higher than those of *Cgfoxl2a-Bs-a* and *Cgfoxl2b-As*. However, only *Cgfoxl2a-Bs-a* and *Cgfoxl2a-Bs-b* were highly expressed in the pituitary. Interestingly, *Cgfoxl2b-As* and *Cgfoxl2b-Bs* exhibited sexually dimorphic pattern with higher expression in ovary compared with testis, whereas *Cgfoxl2a-Bs-a* expression was almost absent in gonads and *Cgfoxl2a-Bs-b* showed similar expression levels between ovary and testis. The divergent expression patterns of gibel carp *foxl2s* imply significantly biased expression of them in adult tissues.

Subsequently, we analyzed their dynamic expression changes in unfertilized eggs, 50% epiboly, hatching fry, and developing ovaries from 10 days posthatching (dph) to 270 dph and mature ovary (fig. 2*B*). Maternal *foxl2as* and *foxl2bs* transcripts were detected in unfertilized eggs and their zygotic products are synthesized in hatching fry. During ovary differentiation and maturation, only a few of *Cgfoxl2a-Bs-a* transcripts were detected. *Cgfoxl2a-Bs-b*, *Cgfoxl2b-As*, and *Cgfoxl2b-Bs* were all abundantly expressed at 25 dph, quickly reached peak values at 35 dph, and then gradually decreased to the lowest values at 190 dph. From 25 to 35 dph, the expression level of *Cgfoxl2a-Bs-b* was higher (2.5–7.1 fold) than those of *Cgfoxl2b-As* and *Cgfoxl2b-Bs*. Along with the maturing of ovary, their expression all mildly increased, and more transcripts of *Cgfoxl2b-As* and *Cgfoxl2b-Bs* were detected than *Cgfoxl2a-Bs-b*.

According to the specific SNPs in three alleles of each *foxl2* genes, we tried to present the expression differences among three alleles through sequencing the amplified fragments (fig. 2*C*). In the developing ovary at 45 dph, more than 92.6% of sequencing clones on average (about 20–30 clones each individual, $n = 3$) belonged to *Cgfoxl2a-B2* and *Cgfoxl2a-B3*, indicating that the expression levels of *Cgfoxl2a-B2* and *Cgfoxl2a-B3* were much higher than that of *Cgfoxl2a-B1*. Although *Cgfoxl2a-B1-a* still kept low expression, *Cgfoxl2a-B1-b* seemed to raise about 4-folds of its expression, making up about a quarter of total *Cgfoxl2a-B1/B2/B3-b* expression in the maturing ovary at 270 dph. The biased expression pattern in developing testis was similar to developing ovary (45 dph), whereas the pattern in maturing testis was remarkably different from those in ovary. *Cgfoxl2a-B2* appeared to play a dominant role, occupying two-thirds of *Cgfoxl2a-B1/B2/B3-b* expression in maturing testis. The three alleles of *Cgfoxl2b-A* and *Cgfoxl2b-B* did not show obviously biased expression in ovary and presented similar expression levels, respectively. In maturing testis, the expression of *Cgfoxl2b-B1* was much more abundant than those of other alleles.

Distinct Cellular Localization of *Cg*Foxl2a and *Cg*Foxl2b during Ovary and Oocyte Development

Two polyclonal antibodies specific for *Cg*Foxl2a and *Cg*Foxl2b were produced and confirmed by Western blot (supplementary fig. S3, Supplementary Material online). Anti-*Cg*Foxl2a antibody can specifically recognize the overexpressing HA-tagged *Cg*Foxl2a-B protein (HA-*Cg*Foxl2a-B) in 293 T cells and not detect HA-*Cg*Foxl2b-A or HA-*Cg*Foxl2b-B proteins and vice versa for anti-*Cg*Foxl2b antibody. The cellular localization of *Cg*Foxl2a and *Cg*Foxl2b proteins were assessed in ovaries from 20 dph to adult by immunofluorescence analysis (fig. 2*D*). At 20 dph, a few of primordial germ cells (PGCs) scattered in the gonadal primordia and were surrounded by somatic cells. Punctate *Cg*Foxl2b immunofluorescence signals were observed in the perinuclear region of PGCs. Three kinds of somatic cells with positive signals in nuclei were distinguished. The first was strongly marked by both *Cg*Foxl2a and *Cg*Foxl2b (indicated by arrowheads), and the second had intensely *Cg*Foxl2a positive signals in the fusiform nucleus (indicated by asterisks). The third had elliptical nuclei with dispersive and star-like signals of *Cg*Foxl2a (indicated by trapezoid). At 45 dph, oogonia massively proliferated and cysts started to form. A few of oogonia differentiated into primary oocytes (PO, I). In the perinuclear region of oogonia and PO, much punctate *Cg*Foxl2b positive signals were observed. At 50 dph, more oogonia differentiated into PO, where *Cg*Foxl2b localized in the perinuclear region and close to chromatins. Several somatic cells scattered and surrounded PO, implying the initiation of follicular lay formation. PO was first surrounded by granulosa cells (indicated by arrowheads) which were coexpressed *Cg*Foxl2a and *Cg*Foxl2b, and then by theca cells (indicated by asterisks) emitted only *Cg*Foxl2a immunofluorescence signals. Along with oogonia differentiation and PO growth (60-89 dph), *Cg*Foxl2b proteins in peripheral area of PO nucleus interspersed into ooplasm, and granulosa cells (indicated by arrowheads) coexpressed *Cg*Foxl2a and *Cg*Foxl2b proteins began to proliferate. Merged imagination clearly discriminated three subpopulations of thecal cells, expressing *Cg*Foxl2a (indicated by asterisks), coexpressing *Cg*Foxl2a/2b (indicated by hexagons) and not expressing *Cg*Foxl2a/2b cell (indicated by pentagons). In maturing ovary, two successive follicular layers, granulosa lay and thecal lay, formed and enclosed vitellogenic oocytes (III) and maturing oocytes (IV). As oocytes grew, *Cg*Foxl2a immunofluorescence signals became weak and *Cg*Foxl2b persisted abundant expression in granulosa cells. In thecal layer surrounding vitellogenic oocytes, about $26.1 \pm 7.4\%$, $8.0 \pm 3.0\%$, and $65.9 \pm 8.9\%$ thecal cells were expressed only *Cg*Foxl2a, coexpressed *Cg*Foxl2a and *Cg*Foxl2b, or expressed neither *Cg*Foxl2a nor *Cg*Foxl2b, respectively. In addition, many *Cg*Foxl2a-expressed cells were observed in the stromal layer throughout ovary development. In testis, very faint *Cg*Foxl2a and *Cg*Foxl2b immunofluorescence signals were observed only in the spermatogonia (SPG).

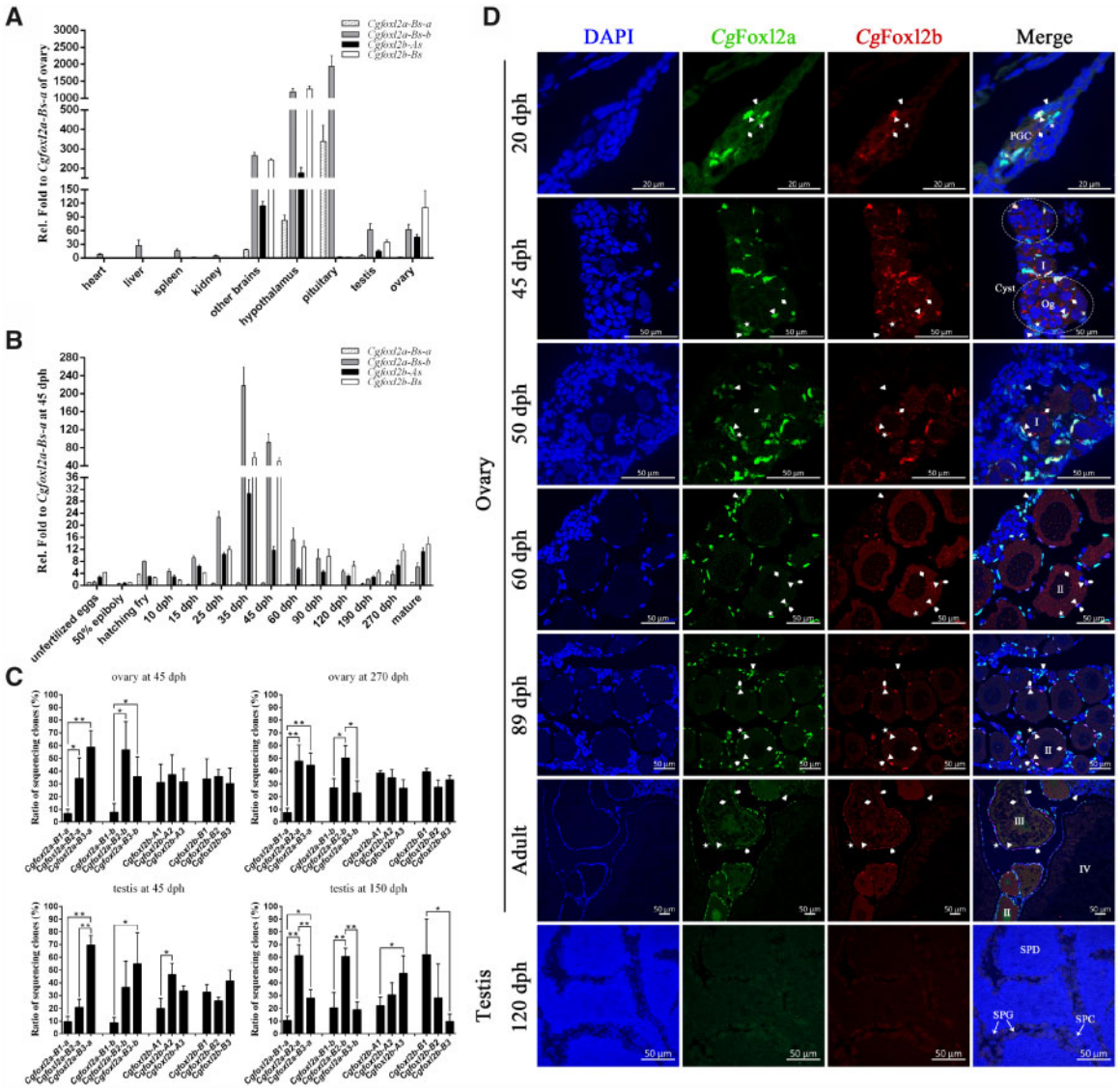

Fig. 2. Divergent expression pattern of gibel carp *foxl2a* and *foxl2b*. (*A*, *B*) qPCR analysis of *Cgfoxl2a-B*, *Cgfoxl2b-A*, and *Cgfoxl2b-B* expression in adult tissue (*A*), unfertilized eggs, 50% epiboly, hatching fry, and ovaries at different developmental stages (*B*). *eef1a1l1* was used as control. Each bar represents mean ± standard deviation ($n = 3$). (*C*) Ratios of sequencing clones of *Cgfoxl2a-B*, *Cgfoxl2b-A*, and *Cgfoxl2b-B* alleles in ovaries and testis at different developmental stages. Asterisks indicate the significant differences ($^*P < 0.05$ and $^{**}P < 0.01$). (*D*) Dynamic codistribution of *Cg*Foxl2a and *Cg*Foxl2b protein in ovary during oogenesis (20 dph to adult) and adult testis revealed by immunofluorescence localization. Green and red fluorescence are stained by *Cg*Foxl2a and *Cg*Foxl2b antiserum, respectively, and blue fluorescence is stained by DAPI. Five kinds of somatic cells can be distinguished in gibel carp ovary, including somatic cell in the stromal layer expressing *Cg*Foxl2a (indicated by trapezoid), granulosa cell coexpressing *Cg*Foxl2a/2b (indicated by arrowheads), thecal cell expressing *Cg*Foxl2a (indicated by asterisks), thecal cell coexpressing *Cg*Foxl2a/2b (indicated by hexagons), and thecal cell not expressing *Cg*Foxl2a/2b (indicated by pentagons). The *Cg*Foxl2b immunofluorescence signals in ooplasm of PGCs, oogonia, primary oocyte (I), growth stage oocyte (II), vitellogenic oocyte (III), and maturing oocyte (IV) are indicated by rhombuses. Bars are shown at bottom-right of the images.

*Cg*Foxl2a-B Deficiency Led to Ovary Development Arrest and Sex Reversal in a Dosage-Dependent Manner

The dynamic expression and distinct cellular localization of *Cg*Foxl2a and *Cg*Foxl2b suggest that their functions might have been diverged. To explore this, we generated *Cgfoxl2a-B*, *Cgfoxl2b-A*, and *Cgfoxl2b-B* singly or simultaneously disrupted gibel carps using CRISPR/Cas9. The targeting site of *Cgfoxl2a-B* was chosen in the second exon to disrupt the FKH domain (supplementary fig. S4*A*, Supplementary Material online). Due to polyploidy nature of gibel carp, a lot of complicatedly mutated genotypes modified at the target sites were detected in the F0 individuals. All of F0 individuals developed normally and grew to fertile females, similar to WT. Two individuals, named as F0-1 and F0-2, were chosen to proliferate by gynogenesis. The sequencing results showed that the mutations of these two F0 individuals both caused a reading frame shift (supplementary fig. S4*C* and *D*, Supplementary Material online).

To exclude the influences of environmental factors on gibel carp sex differentiation, we raised WT individuals and *Cgfoxl2a-B* mutated F1 gynogenetic offspring together to adult in the same cage. Gibel carp became sex mature after raising 1 year. A total of 212 individuals were randomly sampled to identify their genotypes and to analyze their gross morphology and histology of gonads, of which 140 individuals were identified as *Cgfoxl2a-B* mutants with different mutated genotypes. According to the specific SNPs in three alleles of *Cgfoxl2a-B*, the 61 F1 gynogenetic offspring of F0-1 were classified into three mutated genotypes ($Cgfoxl2a\text{-}B^{\Delta 47/\Delta 7+11/\Delta 4+5}$ [$n=5$], $Cgfoxl2a\text{-}B^{\Delta 47/\Delta 23+12/\Delta 2+1}$ [$n=4$], and $Cgfoxl2a\text{-}B^{\Delta 55/\Delta 54/\Delta 25+8}$ [$n=52$]), and the 79 F1 gynogenetic offspring of F0-2 were clustered into six mutated genotypes ($Cgfoxl2a\text{-}B^{\Delta 5/\Delta 39/\Delta 10}$ [$n=16$], $Cgfoxl2a\text{-}B^{\Delta 5/\Delta 39/\Delta 16}$ [$n=12$], $Cgfoxl2a\text{-}B^{\Delta 44/\Delta 42+1/\Delta 18+12}$ [$n=38$], $Cgfoxl2a\text{-}B^{\Delta 11+26/\Delta 11+26/\Delta 15+1}$ [$n=2$], $Cgfoxl2a\text{-}B^{+/\Delta 39/\Delta 10}$ [$n=8$], and $Cgfoxl2a\text{-}B^{+/\Delta 36/\Delta 5}$ [$n=3$]), respectively (fig. 3A and *B*).

The vast majority (95.8%) of WT gibel carp were fertile females (fig. 3A), with ovaries containing a lot of maturing oocytes (IV), vitellogenic oocytes (III), growth stage oocytes (II), and PO (I) (fig. 3C). According to the edited efficiency of three alleles, the mutated genotypes were classified into three groups. The first group (I) included $Cgfoxl2a\text{-}B^{\Delta 47/\Delta 7+11/\Delta 4+5}$ and $Cgfoxl2a\text{-}B^{\Delta 47/\Delta 23+12/\Delta 2+1}$ in which the three alleles all created a premature stop codon and lost FKH domain (fig. 3B). About two-thirds of mutated individuals arrested ovary development at primary oocyte growth stage and the rest developed to males. Compared with WT mature ovary, the arrested ovary is small and translucent with a lot of PO and growth stage oocytes, and only a few of oocytes developed to cortical alveolus stage. The mutated males had normal testis, filling numerous SPG, spermatocytes (SPC), and spermatids (SPD) into testicular lobules (fig. 3C). To confirm the knockout effects of *Cg*Foxl2a-B, the individuals of $Cgfoxl2a\text{-}B^{\Delta 47/\Delta 7+11/\Delta 4+5}$ were sampled to perform immunofluorescence analysis (fig. 4). No *Cg*Foxl2a immunofluorescence signal was observed, implying the disruption of *Cg*Foxl2a-B protein expression in ovary and testis of $Cgfoxl2a\text{-}B^{\Delta 47/\Delta 7+11/\Delta 4+5}$ (fig. 4). Similar to WT, *Cg*Foxl2b proteins were localized in the perinuclear region of PO, nuclei of all granulosa cells and a minority of thecal cells, and SPG. The second group (II) included five mutated genotypes, in which one or two alleles lost FKH domain and the rest alleles presented sense mutation and deletion between N-terminal and FKH domain (fig. 3B and C). Among 120 adult individuals, about 45.0% individuals were males and 11.7% individuals had arrested ovary, whereas others had normal mature ovaries (fig. 3A). All mutated males had normal testis. The fertilization rates and hatching rates were similar to those in control groups (supplementary table S2, Supplementary Material online). Immunofluorescence analysis also confirmed the loss of *Cg*Foxl2a signal (fig. 4). The third group (III) consisted of the rest two mutated genotypes ($Cgfoxl2a\text{-}B^{+/\Delta 39/\Delta 10}$ and $Cgfoxl2a\text{-}B^{+/\Delta 36/\Delta 5}$), possessing WT *Cgfoxl2a-B1* allele, mutated *Cgfoxl2a-B2* allele with sense mutation and deletion between N-terminal and FKH domain and mutated *Cgfoxl2a-B3* allele with premature stop codon (fig. 3B). Two individual of $Cgfoxl2a\text{-}B^{+/\Delta 36/\Delta 5}$ arrested ovary development and the other developed mature females. Among eight individuals of $Cgfoxl2a\text{-}B^{+/\Delta 39/\Delta 10}$, one appears to have arrested ovary, the rest developed to mature males (fig. 3A). Compared with WT ovary, obviously less immunofluorescence *Cg*Foxl2a signals were detected in the arrested ovary of $Cgfoxl2a\text{-}B^{+/\Delta 36/\Delta 5}$.

Mutated *Cgfoxl2a-B* Allele with an Intact FKH Domain Can Activate *Cgcyp19a1a-A* Expression

Due to clinical heterogeneity and haploinsufficiency of human FOXL2 mutations (Verdin and De Baere 2012; Takahashi et al. 2013), we tried to compare the effects of different *Cgfoxl2a-B* mutated alleles on ovary and testis at oogonia or SPG proliferation stage (fig. 5 and supplementary fig. S5, Supplementary Material online). We chose $Cgfoxl2a\text{-}B^{\Delta 55/\Delta 54/\Delta 25+8}$, a mutated genotype having most F1 individuals, to perform further analysis. First, one pair of primers located in the no mutation site was designed to detect the expression of all *Cgfoxl2a-B* alleles. Consistent with above result (fig. 2B), only a few of *Cgfoxl2a-Bs-a* transcripts were detected in the WT and *Cgfoxl2a-B* mutated ovary and testis. $Cgfoxl2a\text{-}B^{\Delta 55/\Delta 54/\Delta 25+8}$ ovaries showed about half *Cgfoxl2a-B1/B2/B3-b* expression level of WT ovary. Although upregulated *Cgfoxl2a-B1/B2/B3-b* expression (7.5-fold) was observed in $Cgfoxl2a\text{-}B^{\Delta 55/\Delta 54/\Delta 25+8}$ testis when it was compared with WT testis, mutated testis had significantly lower *Cgfoxl2a-B1/B2/B3-b* expression (6.3-fold) than that of WT ovary (fig. 5A). The above results indicate that the mutated *Cgfoxl2a-B* alleles exhibited differential expression levels between ovary and testis at early gonadal development stage.

Subsequently, we first compared the subcellular localization of WT and mutated *Cg*Foxl2a-B proteins in order to analyze whether or not the mutated *Cgfoxl2a-B* alleles still have function. WT *Cgfoxl2a-B2*, $Cgfoxl2a\text{-}B1^{\Delta 55}$, $Cgfoxl2a\text{-}B2^{\Delta 54}$, and $Cgfoxl2a\text{-}B3^{\Delta 25+8}$ were linked to green fluorescent protein (GFP) and transfected into HEK293T cells, respectively (fig. 5B). Similar to WT *Cg*Foxl2a-B2 protein, the mutated *Cg*Foxl2a-B proteins containing an intact FKH domain encoded by $Cgfoxl2a\text{-}B2^{\Delta 54}$ localized in the nucleus, implying that they may keep transactivation capacity. The truncated *Cg*Foxl2a-B protein without FKH domain encoded by $Cgfoxl2a\text{-}B1^{\Delta 55}$ and $Cgfoxl2a\text{-}B3^{\Delta 25+8}$ diffusely distributed in the cytoplasm and nucleus.

A lot of studies have revealed the regulative roles of Foxl2 on *cyp19a1* expression (Wang et al. 2007; Bertho et al. 2018). Subsequently, we performed luciferase assays to evaluate the expression of *Cgcyp19a1a* by co-transfection of *Cgcyp19a1a* promoter with WT *Cgfoxl2a-B2*, $Cgfoxl2a\text{-}B1^{\Delta 55}$, $Cgfoxl2a\text{-}B2^{\Delta 54}$, and $Cgfoxl2a\text{-}B3^{\Delta 25+8}$, respectively (fig. 5C and supplementary fig. S6, Supplementary Material online). Compared with the control empty vector, overexpression of WT *Cgfoxl2a-B2* alone could not trigger *Cgcyp19a1a-A* transcription, but coexpression of WT *Cgfoxl2a-B2* and *Cgsf1a-B* significantly activated *Cgcyp19a1a-A* transcription in Crucian carp blastula embryonic cells (CAB) (fig. 5C) and *Epithlioma papulosum cyprinid* cells (EPC) (supplementary fig. S6, Supplementary Material online) cells. The results imply that

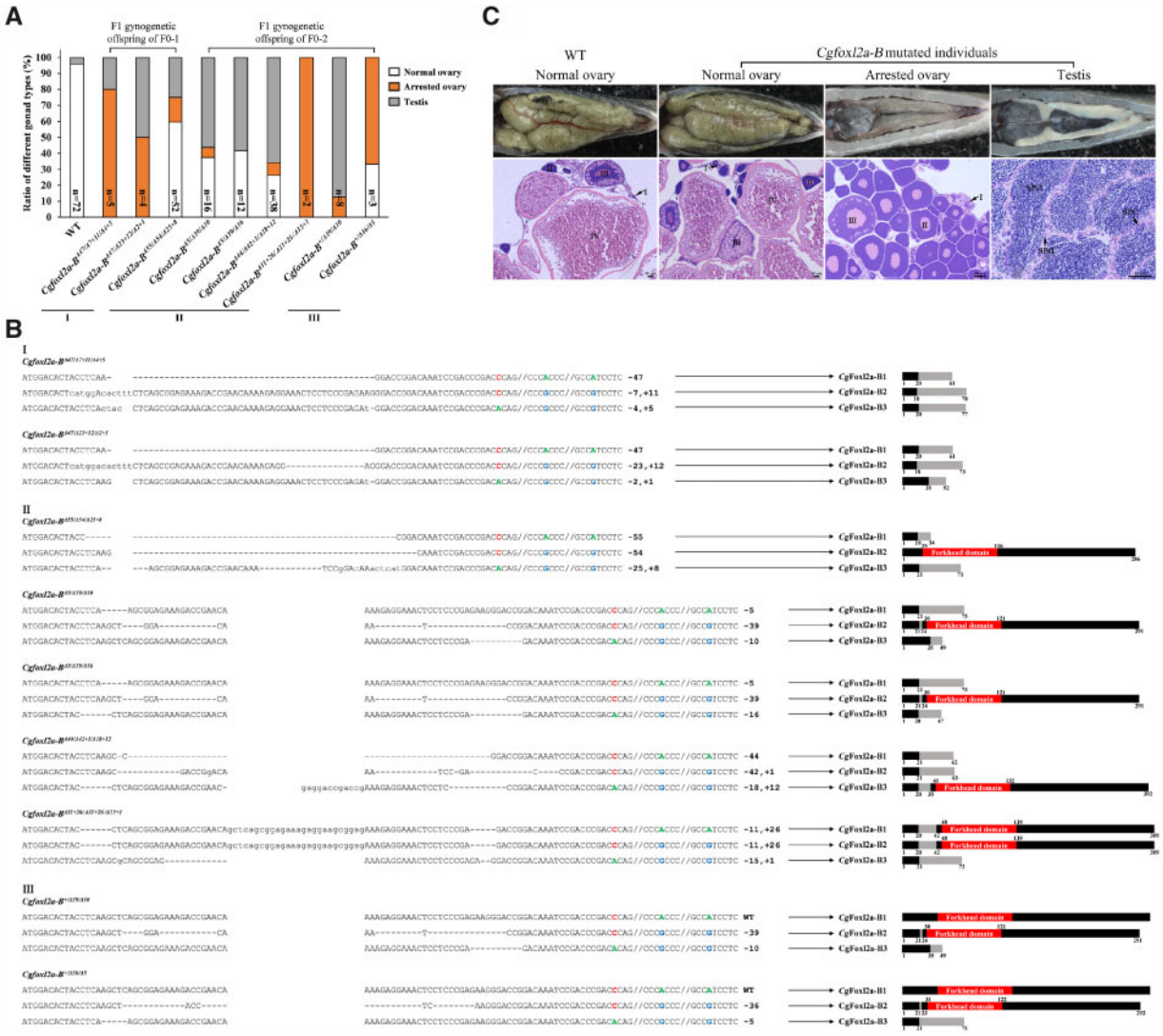

FIG. 3. Disruption of *Cgfoxl2a-B* led to ovary development arrest and complete female to male sex reversal. (*A*) Ratios of normal ovary, arrested ovary, and testis in WT and *Cgfoxl2a-B*-mutated F1 gynogenetic individuals. One hundred and forty *Cgfoxl2a-B*-mutated individuals were clustered into nine mutated genotypes, which classified into three groups (I, II, and III) according to the edited efficiency of three alleles. (*B*) Sequences of *Cgfoxl2a-B* mutations in the nine mutated genotypes. (*C*) Gross morphology and histological examination of adult gonads in WT and *Cgfoxl2a-B* mutants. I, primary oocyte; II, growth stage oocyte; III, vitellogenic oocyte; IV, maturing oocyte. Bars are shown at bottom-right of the images.

Cgfoxl2a-B2 can enhance SF1-activated *Cgcyp19a1a-A* expression. Although *Cgfoxl2a-B1*$^{\Delta 55}$ and *Cgfoxl2a-B3*$^{\Delta 25+8}$ had no effect, overexpression of *Cgfoxl2a-B2*$^{\Delta 54}$ and *Cgsf1a-B* can activate *Cgcyp19a1a-A* expression. In addition, overexpression of *Cgsf1a-B* significantly inhibited *Cgcyp19a1a-B* expression, which can be rescued by coexpression with WT *Cgfoxl2a-B2* or *Cgfoxl2a-B2*$^{\Delta 54}$. The results indicate that CgFoxl2a-B2$^{\Delta 54}$ possess transcriptional activation capacity. Consistent with sexually dimorphic expression of *Cgfoxl2a-Bs-b*, *Cgcyp19a1as* also had higher expression in ovary than that in testis at oogonia or SPG proliferation stage. Meantime, *Cgdmrt1s* was downregulated its expression in ovary (fig. 5A). Taken together the above results, we speculate that the downregulated expression of *Cgfoxl2a-Bs-b* in some gonad may result in lower expression of *Cgcyp19a1as*, which is not sufficient to initiate ovary development.

We also compared the dynamic expression changes of a dozen of important genes involved in gonadal development, including germ cell markers (*vasa* and *dnd*) (Xu et al. 2005; Liu et al. 2015), testis differentiation-related genes (*dmrt1* and *sox9b*) (Forconi et al. 2013; Li, Li, et al. 2014), oocyte-derived factor (*gdf9*) (Liu et al. 2012), and genes in steroidogenic pathway (*sf1a*, *cyp11a1*, *cyp17a1*, *cyp17a2*, *cyp19a1a*, and *srd5a1*) (Payne and Hales 2004; Park and Jameson 2005; Vizziano et al. 2007; Iwade et al. 2008; Kayampilly et al. 2010; Yang et al. 2017) in WT ovary, mutated ovary and testis (fig. 5D). Except *cyp17a1* and *cyp17a2*, all other genes have two divergent homeologs, which showed significantly biased expression (supplementary fig. S7, Supplementary Material online). Compared with their expression in ovaries (WT and *Cgfoxl2a-B*$^{\Delta 55/\Delta 54/\Delta 25+8}$ ovaries), *dmrt1s*, *sox9bs*, *sf1as*, *cyp11a1s*, *vasas*, *cyp17a1-B*, and *cyp17a2-B* remarkably increased, but *dnds*, *cyp19a1a-A*, *gdf9s*, and *srd5a1s*

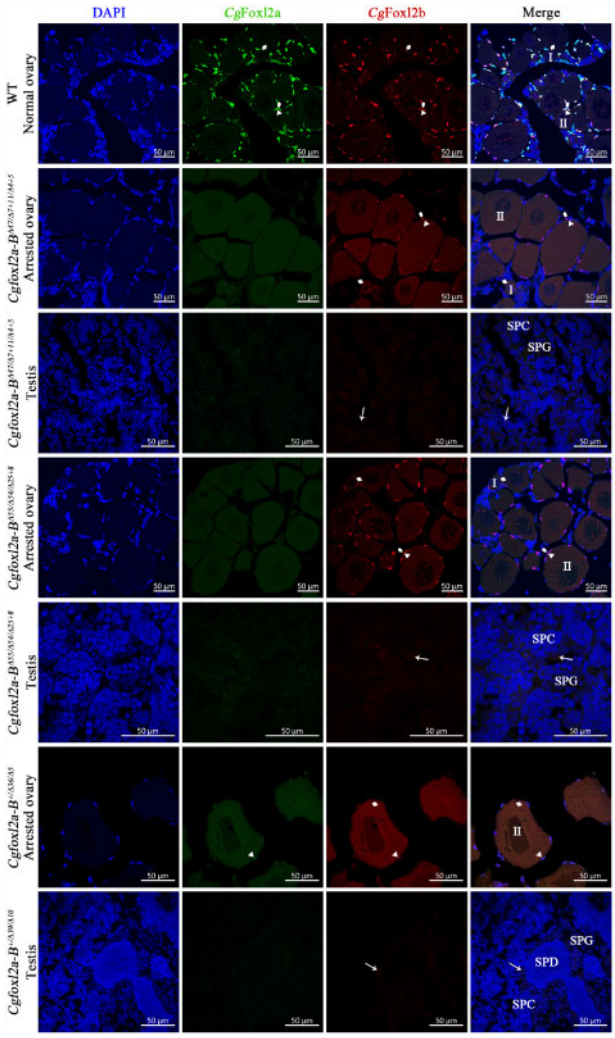

FIG. 4. Immunofluorescence localization of *Cg*Foxl2a and *Cg*Foxl2b proteins in gonads of WT, *Cgfoxl2a-B*$^{\Delta47/\Delta7+11/\Delta4+5}$, *Cgfoxl2a-B*$^{\Delta55/\Delta54/\Delta25+8}$, *Cgfoxl2a-B*$^{+/\Delta36/\Delta5}$, and *Cgfoxl2a-B*$^{+/\Delta39/\Delta10}$-mutated individuals. No or little *Cg*Foxl2a immunofluorescence signal was observed, and *Cg*Foxl2b immunofluorescence signals were observed in oogonia and PO (indicated by rhombuses), granulosa cell (indicated by arrowheads), thecal cells (indicated by hexagons), and SPG (indicated by arrows). Bars are shown at bottom-right of the images.

decreased in *Cgfoxl2a-B*$^{\Delta55/\Delta54/\Delta25+8}$ testis at 89 dph. In addition, *Cgfoxl2b-A* and *Cgfoxl2b-B* showed similar expression between WT and *Cgfoxl2a-B*$^{\Delta55/\Delta54/\Delta25+8}$ gonads (fig. 5*D*).

Complete Disruption of *Cgfoxl2b-A* and *Cgfoxl2b-B* Resulted in Germ Cell Depletion

We also chose conserved sites in the second exon as targeting sites of CRISPR/Cas9 to simultaneously disrupt *Cgfoxl2b-A* and *Cgfoxl2b-B* (supplementary fig. S8*A*, Supplementary Material online). The F0-mutated *Cgfoxl2b-A* and *Cgfoxl2b-B* individuals were cocultured with WT in the same cage and randomly sampled at each stage from 45 dph to mature adult. Compared with WT gibel carp (97.6% of individuals were females, $n = 84$), all of *Cgfoxl2b-A* and *Cgfoxl2b-B* double-mutated F0 individuals ($n = 59$) seemed to have abnormal ovary development, possessing delayed ovary ($n = 36$), germ cell-depleted gonad ($n = 14$), ovotestis ($n = 6$), and testis ($n = 3$) (fig. 6*A* and *B*).

At oogonia proliferation and differentiation stage (45–60 dph, stage I), WT ovaries enlarged, and oogonia rapidly proliferated and started to differentiate to PO. Among 16 F0-mutated *Cgfoxl2b-A*/*Cgfoxl2b-B* individuals, seven, eight, and one individuals had delayed ovary, gonad without germ cell and testis. In comparison with normal ovary, the delayed ovary still retained in oogonia proliferation stage. The gonads without germ cells remained thin thread-like shape, and no PGCs and oogonia were found in the histological sections (fig. 6*C*), which were confirmed by no positive immunofluorescent signal of Vasa detected in their gonad sections (fig. 6*D*). Along with the oocyte growth (80–110 dph, stage II), overwhelming majority of WT gonads (95.5%, $n = 22$) developed into typical ovaries with a lot of PO (I) and growth stage oocytes (II). However, the ratios of delayed ovary, germ cell-depleted gonad, ovotestis, and testis in mutants were 13:4:1:0. The delayed ovaries were still at the oogonia proliferation stage. Gonadal somatic cells proliferated a little in germ cell-depleted gonads, and a huge number of PO (I), growth stage oocyte (II), and spermatogenic cysts containing SPG, SPC, and SPD were mixed in the ovotestis. None of *Cgfoxl2b-A* and *Cgfoxl2b-B* mutants developed mature female and spawned eggs (180–360 dph, stage III). The ratios of arrested ovary, germ cell-depleted gonad, ovotestis, and testis were 16:2:5:2. The results of F0-mutated *Cgfoxl2b-A*/*Cgfoxl2b-B* individuals are distinct from the normal ovary development in the F0-mutated *Cgfoxl2a-B* individuals, which indicates that *Cg*Foxl2b might play a dominant role in gibel carp oogenesis.

Due to no fertile female obtained in this study, we can only randomly select three F0 individuals with different gonad phenotypes to analyze their genotypes. We also discriminated three alleles of *Cgfoxl2b-A* and *Cgfoxl2b-B* according to their specific SNPs. The mutation rates of F0 individuals with germ cell-depleted gonads were the highest, sequentially followed by F0 individuals having testis, ovotestis, and delayed ovaries, which seemed to positively associate with the severity of ovary defects or changes (fig. 6*E* and supplementary table S3 and figs. S9–S12, Supplementary Material online). For example, no WT allele of *Cgfoxl2b-B* was found in the three mutated individuals possessing germ cell-depleted gonad, and their vast majority of sequencing clones (97.1–100.0%) of *Cgfoxl2b-A* were identified as mutated types (supplementary fig. S10, Supplementary Material online). In addition, all of mutated *Cgfoxl2b-A* and *Cgfoxl2b-B* alleles contain frameshift mutations in FKH domain. The results indicate that complete disruption of *Cgfoxl2b-A* and *Cgfoxl2b-B* led to the depletion of germ cell in gibel carp. The mutated individuals having testis also showed highly mutation rates. However, compared with mutated genotypes in germ cell-depleted gonad, a little more WT *Cgfoxl2b-A* allele or some mutated *Cgfoxl2b-A* alleles with intact FKH domain were detected in these mutated individuals with testis (supplementary fig. S12, Supplementary Material online). The average mutation rates of F0 individuals with ovotestis were 76.5 ± 1.3% of *Cgfoxl2b-A* alleles and 54.3 ± 14.0% of *Cgfoxl2b-B* alleles, which were lower than those of mutants with germ cell-depleted gonad

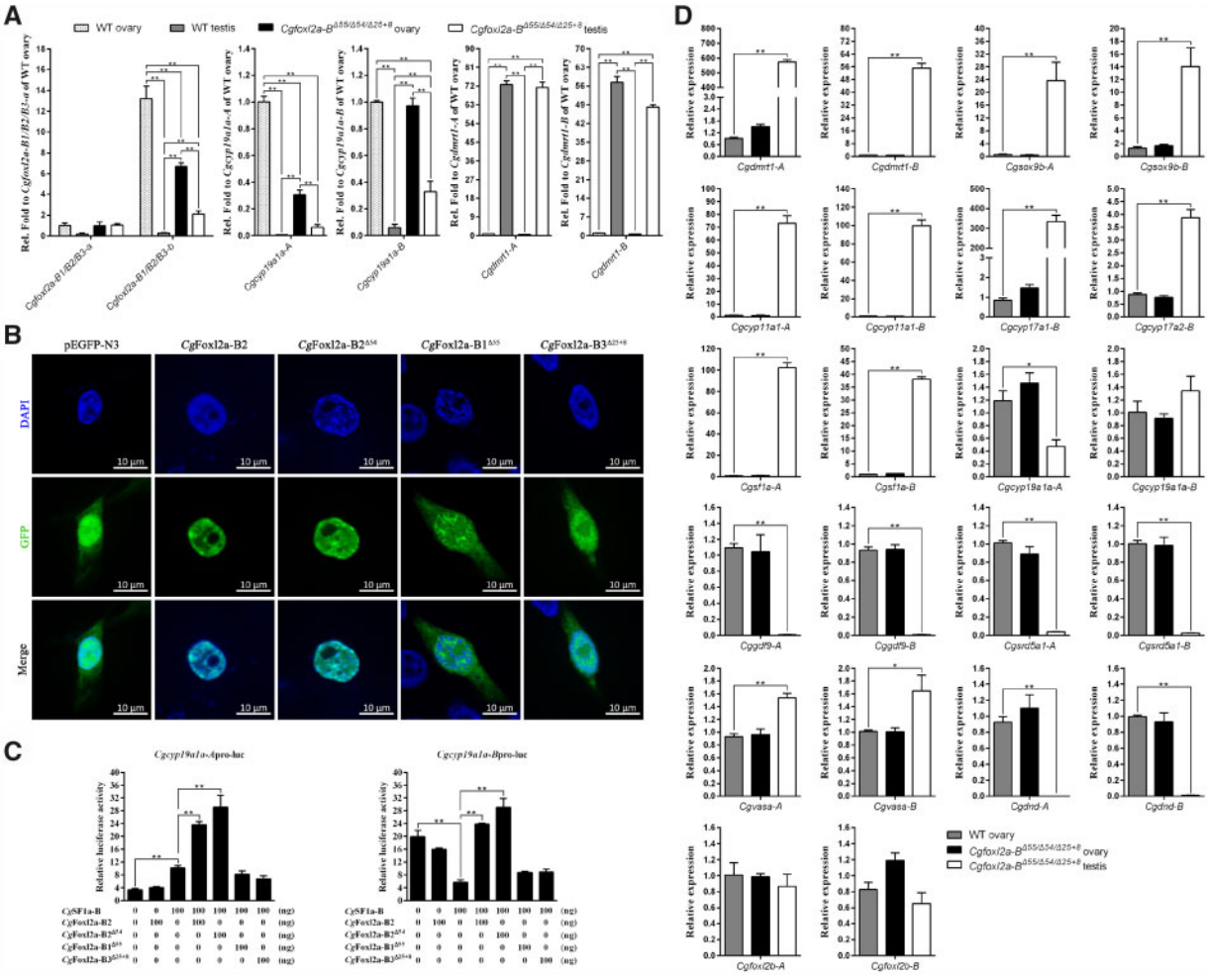

Fig. 5. Mutated *Cgfoxl2a-B* allele with an intact FKH domain keep transactivation and transcriptional activation capacity. (*A*) Total expression level of *Cgfoxl2a-B1/B2/B3*, *Cgcyp19a1a-A*, *Cgcyp19a1a-B*, *Cgdmrt1-A*, and *Cgdmrt1-B*. The asterisks indicate the significant differences (**$P < 0.01$). (*B*) Subcellular localization of WT and mutant *Cg*Foxl2a-B proteins. Nuclear was stained with DAPI and *Cg*Foxl2a-B protein was fused with GFP. Bars are shown at bottom-right of the images. (*C*) Effect of WT and mutated *Cg*Foxl2 proteins on *Cgcyp19a1a-A* and *Cgcyp19a1a-B* promoter activity. WT or mutated *Cgfoxl2a-B* expression vectors were cotransfected into CAB cells with *Cgcyp19a1a* promoter construct and/or *Cgsf1a-B* expression vectors. pRL-TK was used to normalize the expression level. The luciferase activities were detected at 24 h posttransfection. Results are the mean ± SD of triplicate transfections. The asterisks indicate the significant differences (**$P < 0.01$). (*D*) Expression levels of several key genes involved in gonadal development at 89 dph. *eef1a1l1* was used as the normalizer. Gene expression levels are relative to that of WT ovary. Each bar represents mean ± SD ($n = 3$). Asterisks indicate the significant differences (*$P < 0.05$ and **$P < 0.01$).

or testis but higher than those of mutants with delayed ovary (64.2 ± 19.4% of *Cgfoxl2b-A* alleles and 51.5 ± 2.4% of *Cgfoxl2b-B* alleles) (supplementary figs. S9–S12, Supplementary Material online).

Similarly, immunofluorescence localization of *Cg*Foxl2a and *Cg*Foxl2b proteins were analyzed in the F0 individuals with different gonad phenotypes to confirm the knockout effects of *Cg*Foxl2b (fig. 7). Compared with WT ovaries, no *Cg*Foxl2b immunofluorescence signal was observed in the somatic cells of delayed ovary, germ cell-depleted gonad, ovotestis, and testis. However, punctate *Cg*Foxl2b immunofluorescence signals still retained in the oogonia and PO perinuclear region of delayed ovary and ovotestis.

Compensation of *Cgfoxl2a* in Germ Cell-Depleted Gonad of F0 Mutated *Cgfoxl2b-A*/*Cgfoxl2b-B* Individuals Could Not Rescue the Defects

We also analyzed the dynamic expression changes of above genes in F0-mutated *Cgfoxl2b-A*/*Cgfoxl2b-B* individuals (fig. 8). We first focused on their dynamic changes in germ cell-depleted gonad, which was induced by the complete disruption of *Cgfoxl2b-A* and *Cgfoxl2b-B* (supplementary table S3 and fig. S10, Supplementary Material online). None of *vasas* and *dnds* transcripts was detected in the germ cell-depleted gonad (fig. 8). Taking together no Vasa protein detected by immunofluorescent analysis (fig. 6*D*), the results confirmed the complete depletion of germ cell. Compared with WT ovary, delayed ovary and ovotestis, the five testis differentiation-related or androgen-producing genes (*dmrt1s*, *sox9bs*, *sf1as*, *cyp11a1s*, and *cyp17a1-B*) all showed dramatic

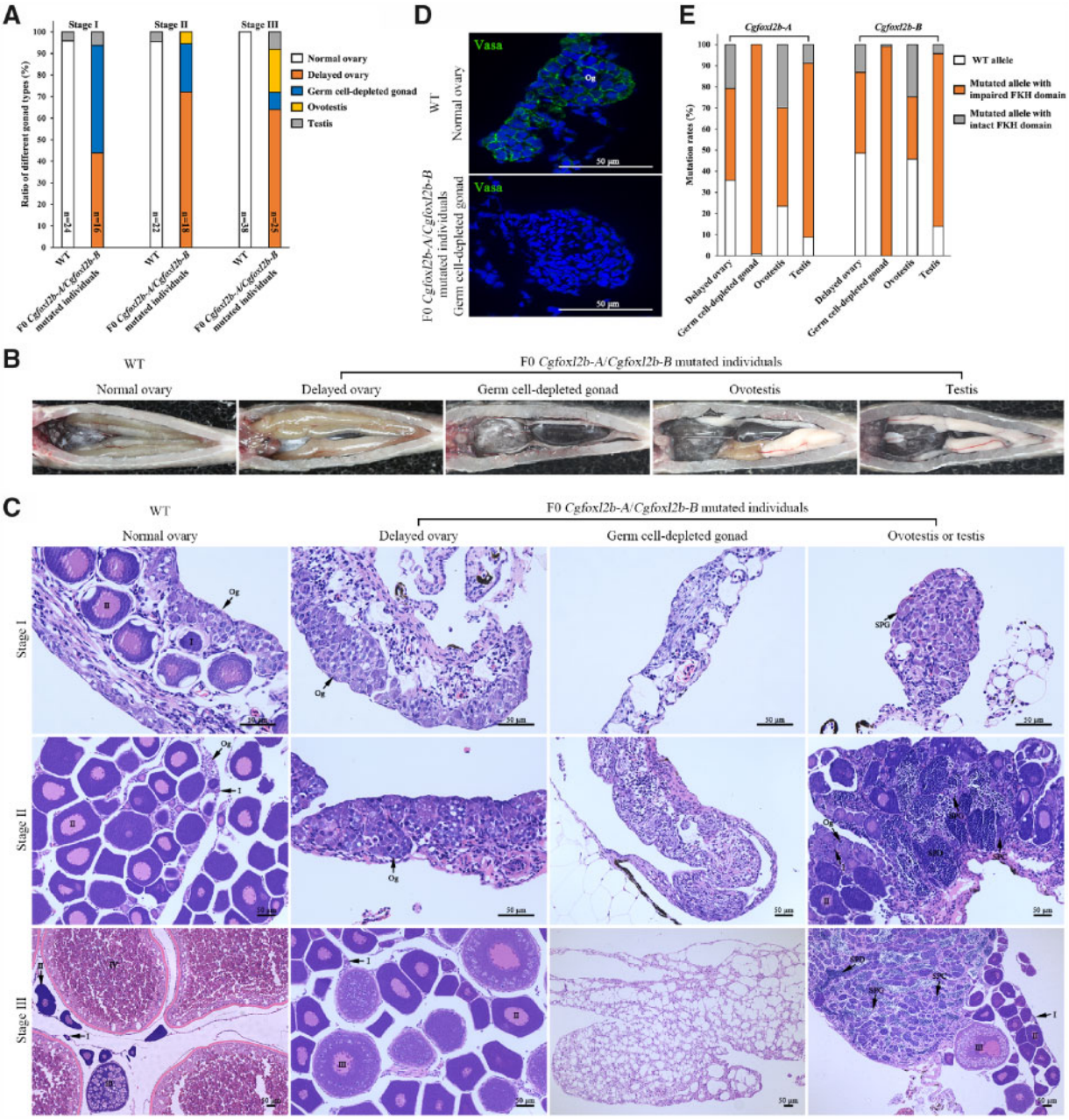

Fig. 6. Complete disruption of *Cgfoxl2b-A* and *Cgfoxl2b-B* led to the depletion of germ cell in gibel carp. (*A*) Ratios of normal ovary, delayed ovary, germ cell-depleted gonad, ovotestis, and testis in WT and F0 *Cgfoxl2b-A*/*Cgfoxl2b-B*-mutated individuals. (*B*) Gross morphology and histological examination of adult gonads in WT and F0 *Cgfoxl2b-A*/*Cgfoxl2b-B*-mutated individuals. (*C*) Histological examination of gonads in WT and *Cgfoxl2b-A*/*Cgfoxl2b-B*-mutated individuals at three different stages (45–60, 80–110, and 180–360 dph). I, primary oocyte; II, growth stage oocyte; III, vitellogenic oocyte; IV, maturing oocyte. Bars are shown at bottom-right of the images. (*D*) Histological examination of gonads in WT and mutated *Cgfoxl2b-A*/*Cgfoxl2b-B* individuals at 45 dph. Green and blue fluorescences are stained by Vasa antiserum and DAPI, respectively. (*E*) Mutated ratios of F0 *Cgfoxl2b-A*/*Cgfoxl2b-B* individuals with delayed ovary, germ cell-depleted gonad, ovotestis, and testis.

upregulation expression, whereas the female-biased genes (*gdf9s* and *srd5a1s*) were remarkably downregulated expression in germ cell-depleted gonad similar to those in testis. The results implied that the germ cell-depleted gonad developed testis-like gonads without spermatogenic cells, consistent with our previous study in which germ cells was depleted by *dnd* morpholino-mediated knockdown approach (Liu et al. 2015). Additionally, *dmrt1s*, *sox9b-B*, *sf1as*, *cyp11a1-B*, and *cyp17a1-B* raised their expression in germ cell-depleted gonad along with gonad development. *cyp19a1as* were remarkably upregulated their expression at oogonia proliferation and differentiation stage (I). Significantly, much more abundant *Cgfoxl2a-Bs* transcripts (3.3–25.3-folds vs. WT ovary) were detected, indicating the compensatory increase of *Cgfoxl2a-Bs* in the germ cell-depleted gonad (fig. 8).

The normal ovary of WT and delayed ovary of F0 mutated *Cgfoxl2b-A*/*Cgfoxl2b-B* individuals showed similar expression patterns of all analyzed genes. The expression levels of testis

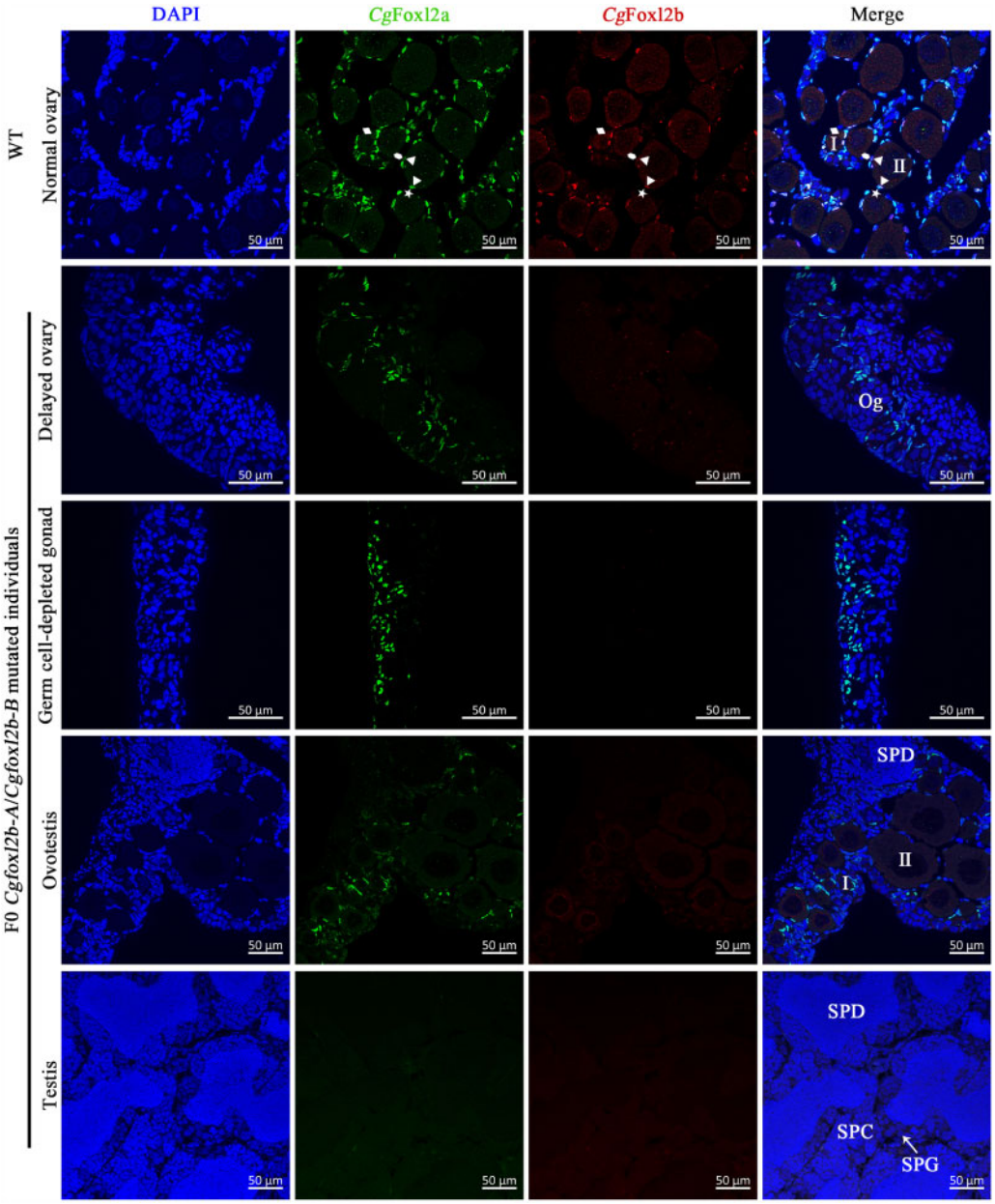

FIG. 7. Immunofluorescence localization of *Cg*Foxl2a and *Cg*Foxl2b proteins in gonads of WT and F0 *Cgfoxl2b-A* and *Cgfoxl2b-B*-mutated gibel carp individuals. No *Cg*Foxl2b immunofluorescence signal was observed in the somatic cells of delayed ovary, germ cell-depleted gonad, ovotestis, and testis. Punctate *Cg*Foxl2b immunofluorescence signals still retained in the oogonia and PO perinuclear region of delayed ovary and ovotestis.

differentiation-related or androgen-producing genes in ovotestis lied halfway in between those of testis and ovary (fig. 8).

More Serious Defects Observed in the *Cgfoxl2a-B*, *Cgfoxl2b-A*, and *Cgfoxl2b-B* Triple-Mutated Individuals

The F0 individuals simultaneously mutated *Cgfoxl2a-B*, *Cgfoxl2b-A*, and *Cgfoxl2b-B* were also obtained by coinjection their specific sgRNAs with Cas9 mRNA. Similar to the *Cgfoxl2b-A* and *Cgfoxl2b-B* double mutants, all of *Cgfoxl2a-B*, *Cgfoxl2b-A*, and *Cgfoxl2b-B* triple mutants ($n = 59$) had aberrant ovary development (supplementary fig. S13, Supplementary Material online). The ratios of mutated individuals with delayed ovary, germ cell-depleted gonad, ovotestis, and testis were 50.8, 20.3, 11.9, and 17.0%, respectively. Compared with *Cgfoxl2b-A* and *Cgfoxl2b-B* mutated individuals (15.3% with ovotestis and testis), more F0 individuals with mutated *Cgfoxl2a-B*, *Cgfoxl2b-A*, and *Cgfoxl2b-B* (28.9%) occurred partial or complete ovary to testis sex reversal. Especially, the ratio of complete sex reversal in F0-mutated *Cgfoxl2a-B*, *Cgfoxl2b-A*, and *Cgfoxl2b-B* individuals (17.0%) was significantly higher than that of *Cgfoxl2b-A* and *Cgfoxl2b-B* individuals (5.1%). The latter is a little higher than that of WT (2.4%). Similar to F0-mutated *Cgfoxl2b-A* and *Cgfoxl2b-B* individuals, no fertile mutated *Cgfoxl2a-B*, *Cgfoxl2b-A*, and *Cgfoxl2b-B* female was obtained. We analyzed the mutation rates of F0 individuals. The mutation rates of F0-mutated *Cgfoxl2a-B*, *Cgfoxl2b-A*, and *Cgfoxl2b-B* also appeared to positively correlate with the severity of ovary defects or changes (supplementary table S4 and figs. S14–S17, Supplementary Material online). The disruption of

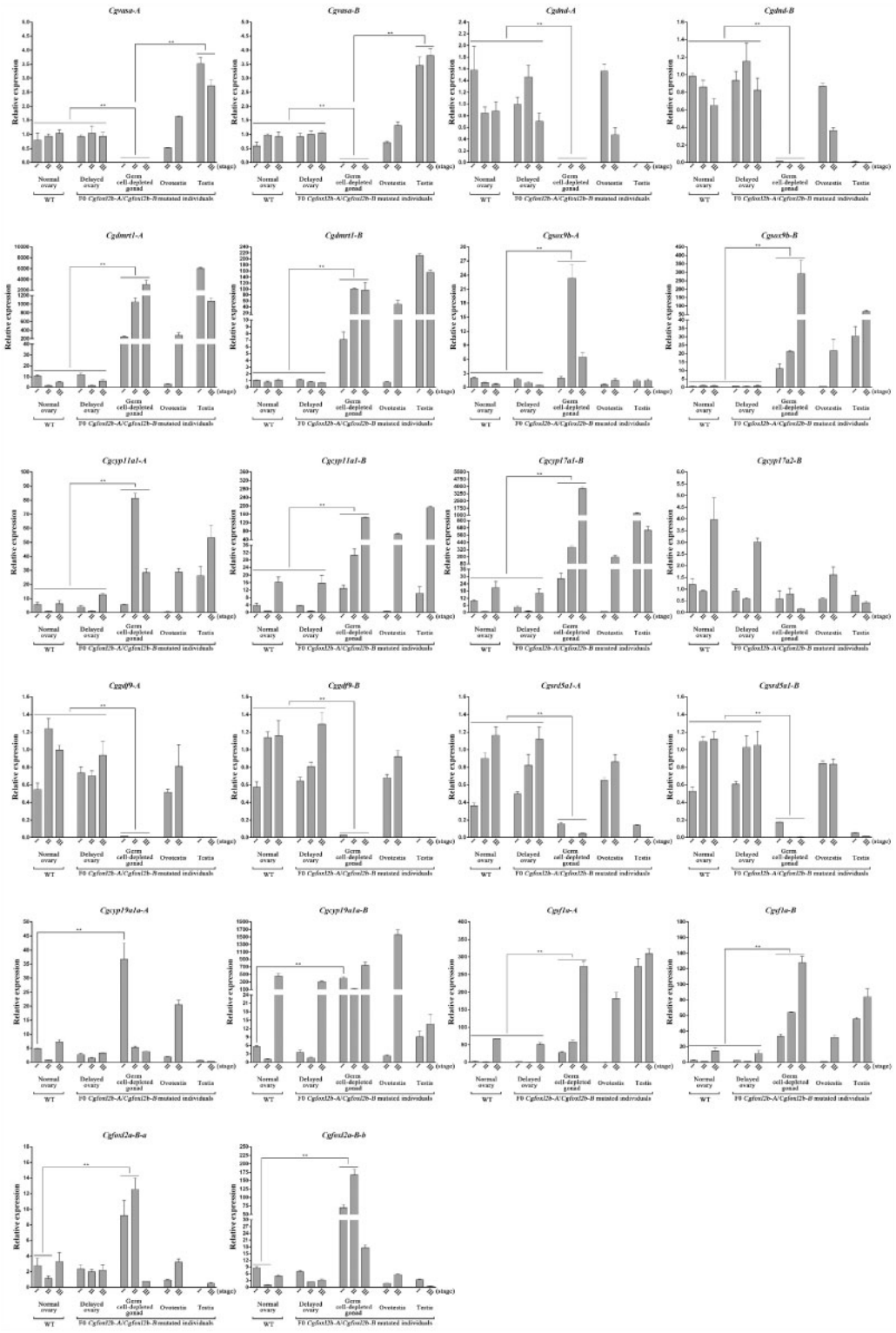

FIG. 8. qPCR analyses of key genes involved in gonadal development in WT ovaries and delayed ovary, germ cell-depleted gonad, ovotestis, and testis of F0 *Cgfoxl2b-A*- and *Cgfoxl2b-B*-mutated individuals at three different stages (45–60, 80–110, and 180–360 dph). *eef1a1l1* was used as the normalizer. Gene expression levels are relative to that of WT ovary at stage II. Each bar represents mean ± SD. Asterisks indicate the significant differences (**$P < 0.01$).

*Cg*Foxl2a and *Cg*Foxl2b expression were also confirmed by immunofluorescence analysis (supplementary fig. S18, Supplementary Material online). No *Cg*Foxl2a and *Cg*Foxl2b immunofluorescence signal was observed in germ cell-depleted gonad. However, faint *Cg*Foxl2a and *Cg*Foxl2b positive signals were detected in delayed ovary and ovotestis. All analyzed genes showed similar dynamic expression changes in the simultaneous disruption of *Cgfoxl2a-B*/*Cgfoxl2b-A*/*Cgfoxl2b-B*

F0-mutated individuals to F0-mutated *Cgfoxl2b-A*/*Cgfoxl2b-B* individuals (supplementary fig. S19, Supplementary Material online).

Discussion

With the explosion of genome sequencing, the importance of polyploidy and postpolyploid diploidization (PPD) in increasing genome complexity, variability, and diversity has been widely discussed later (Van de Peer et al. 2009, 2017; Cheng et al. 2018; Clark and Donoghue 2018; Mandakova and Lysak 2018). In this study, we first identified 12 gibel carp *foxl2* cDNAs, belonging to three *foxl2* genes (*Cgfoxl2a-B*, *Cgfoxl2b-A*, and *Cgfoxl2b-B*) located on three chromosomes of *Cg*B15, *Cg*A2, and *Cg*B2, respectively (fig. 1). Thus, here we presented a typical case to show the diversification of homeologs and alleles in a recurrent hexaploid animal. In addition, most of genes analyzed in this study (figs. 5 and 8 and supplementary fig. S19, Supplementary Material online) and our previous study (Mou et al. 2018) have two divergent homeologs, indicating an allo-polyploidy event occurred in the evolution of gibel carp. Consistent with our previous studies about the identification of *bmp15* and *nanos2* (Jiang et al. 2020; Zhang et al. 2020), three alleles with high identities ($\geq$99.0%) of each *foxl2* gene were identified in this study, implying an auto-polyploidy event occurred in the evolution of gibel carp.

The complex process of PPD, including chromosomal loss/rearrangement, biased gene retention/loss, gene conversion/chimera/fusion, gene sub-/neofunctionalization, biased gene expression and coexpression networks, transposon reactivation, and epigenetic reprogramming, might generate evolutionarily advantageous genomic changes to shape a novel genome of paleopolyploid or new diploid (Doyle et al. 2008; Xiong et al. 2011; Song and Chen 2015; Yang et al. 2016; Edger et al. 2017; Ramirez-Gonzalez et al. 2018). Two *foxl2* paralogs, *foxl2a* and *foxl2b* resulting from Ts3R, retained in many basal teleost or one of them lost in other teleost (Bertho et al. 2016; Yang et al. 2017). In this study, we did not detect *foxl2a-A* in gibel carp and crucian carp genomes, implying the loss of *foxl2a-A* gene in the ancestor of *Carassius* complex after allopolyploidy. Moreover, only a few of genes lost after 5R ploidy event suggested that gibel carp might just step into the process of PPD owing to its relatively short evolutionary history.

The biased gene expression was observed not only between *Cgfoxl2a* and *Cgfoxl2b* but also between *Cgfoxl2b-A* and *Cgfoxl2b-B*. Using qPCR, we also presented biased expression pattern of three alleles. Similar to zebrafish *foxl2a* and *foxl2b* (Yang et al. 2017), *Cgfoxl2a* and *Cgfoxl2b* showed sequential expression (fig. 2*B* and *D*). Altogether with other studies, *foxl2* female-biased and predominant in granulosa expression is conserved and incontrovertible throughout vertebrate (Bertho et al. 2016). Besides granulosa cells, whether thecal cells, oocytes, or other somatic cells express Foxl2 or not seems to be species specific (Govoroun et al. 2004; Pisarska et al. 2004). Gibel carp Foxl2a and Foxl2b proteins showed distinct cellular localization from zebrafish and medaka (*Oryzias latipes*) (fig. 2*D*). Medaka has only one copy of *foxl2* gene and their *foxl2b* copy was lost during evolution. Both zebrafish Foxl2a and medaka Foxl2 were detected in the follicular cells surrounding previtellogenic oocytes and vitellogenic oocytes, not in early oocytes (Herpin et al. 2013; Caulier et al. 2015). *Cg*Foxl2a and/or *Cg*Foxl2b are expressed in the nuclei of granulosa cells and theca cells, and somatic cells in stromal layer at the initial stage of follicular layer formation, implying their important roles in folliculogenesis. Interestingly, three subpopulations of thecal cells were identified. In addition, we observed abundant *Cg*Foxl2b proteins distributed in oogonia and PO, which is similar to medaka Foxl2 proteins (Herpin et al. 2013). The expression of Foxl2 proteins in oogonia and PO implies their direct roles in early oogenesis, independent to their roles in cell communication between oocytes and follicular cells. Therefore, our study provides a clear example to show biased and divergent expression and cellular localization of two teleost paralogs. The results also indicate that *Cg*Foxl2a and *Cg*Foxl2b might display function partition during gibel carp oogenesis.

During ovary development, granulosa cells and theca cells form two layers of ovarian follicle. The interactions among granulosa cells, theca cells, and oocytes are pivotal to folliculogenesis, steroidogenesis, and female oogenesis (Jagarlamudi and Rajkovic 2012; Richards et al. 2018). *Foxl2* is one of the earliest known markers of granulosa cell differentiation (Cocquet et al. 2002; Schmidt et al. 2004). Although a few reports described morphological folliculogenesis in teleost species through histological and ultrastructural observation (Grier 2000, 2012; Grier et al. 2009; Quagio-Grassiotto et al. 2011), the studies on the process of folliculogenesis traced by granulosa cell or theca cell marker genes were scarce. By using two antibodies specific for *Cg*Foxl2a and *Cg*Foxl2b, respectively, we can precisely identify granulosa cells, thecal cells, and their precursor cells. When oogonia differentiate into PO, a few of granulosa cells coexpressed *Cg*Foxl2a and *Cg*Foxl2b directly attach to meiotic oocytes. Meanwhile, theca cells expressed *Cg*Foxl2a are first recruited to the edge of cysts with oogonia and PO and then encompass granulosa cells. Interestingly, the somatic cells in the stromal layer have elliptical nuclei with star-like signals of *Cg*Foxl2a, whereas theca cells are expressed more abundant *Cg*Foxl2a proteins in their fusiform nuclei. The results suggest that thecal cells recruited from the stromal layer to thecal layer seem to undergo morphological differentiation of nuclei. Along with oocytes grow, granulosa cells proliferate and form a regular and successive monolayer, in which *Cg*Foxl2b proteins persist abundant and *Cg*Foxl2a expression decrease. Simultaneously, three subpopulations of thecal cells, expressing *Cg*Foxl2a, coexpressing *Cg*Foxl2a/2b, and not expressing *Cg*Foxl2a/2b cells, recruit from the stromal layer and form successive thecal lay. Thereafter, granulosa cells and theca cells develop two layers of follicular cells (fig. 9*A*).

The complicated and crucial roles of *Foxl2* in ovary development and maintenance have been well documented in mammals (Crisponi et al. 2001; Uhlenhaut et al. 2009; Boulanger et al. 2014) and three teleost fishes (Yang et al. 2017; Zhang et al. 2017; Bertho et al. 2018). Gibel carp is able to reproduce all female offspring by gynogenesis. Thus, we

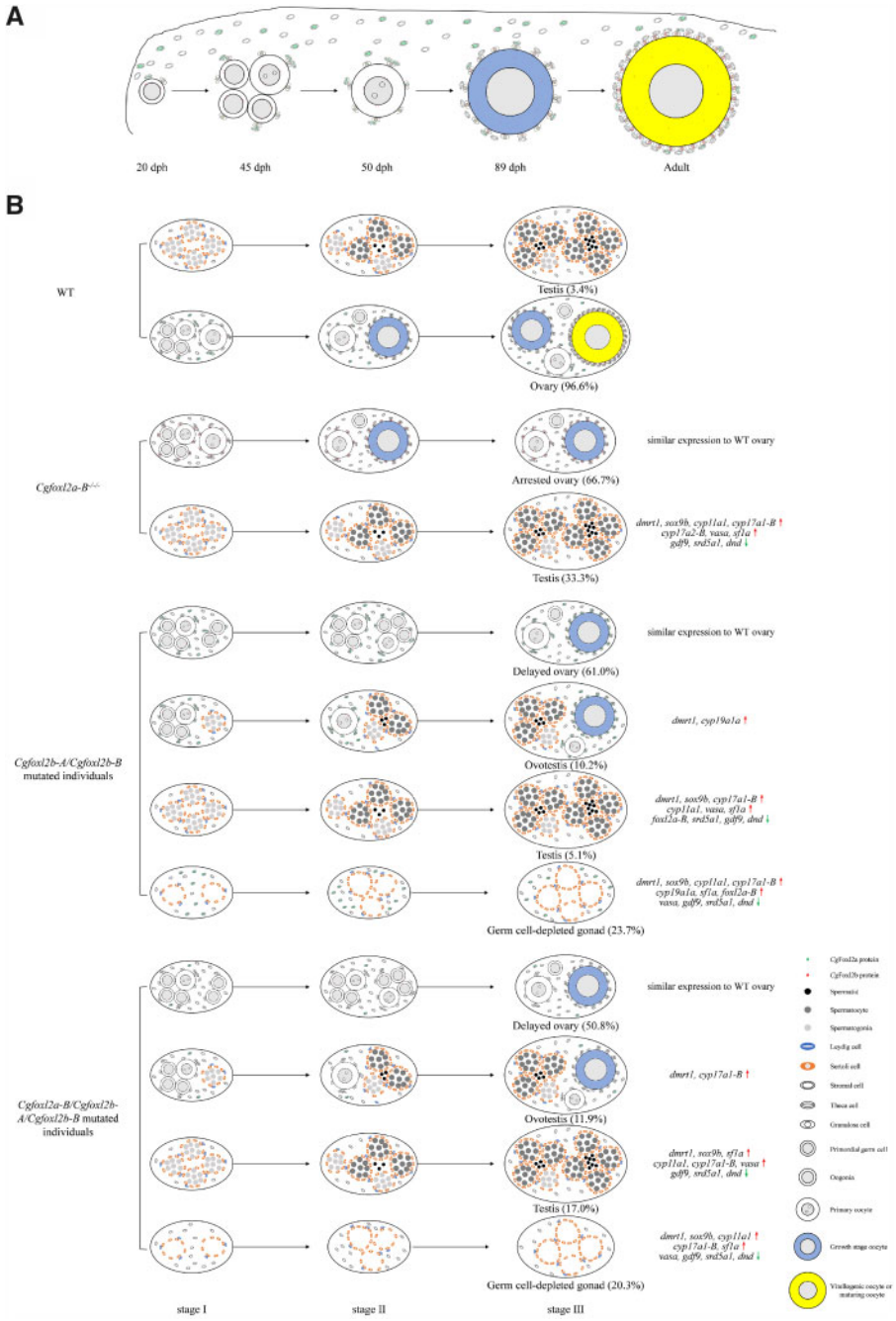

Fig. 9. Schematic diagram of folliculogenesis (*A*) and cooperative regulation between *Cgfoxl2a* and *Cgfoxl2b* (*B*) in gibel carp ovary development. Different granulosa cells, thecal cells, and their precursor cells are distinguished by expression of *Cg*Foxl2a (green) and *Cg*Foxl2b (red) proteins, respectively. Different types of gonads, including WT ovary, delayed ovary, germ cell-depleted gonad, ovotestis, and testis, different gonadal development-related genes and their upregulation and downregulation expressions, are indicated in detail.

speculate that *foxl2* may act as dominant female-determining transcription factor in unisexual species. In this study, we successfully edited multiple *foxl2* homeologs and/or alleles in gibel carp by using CRISPR/Cas9. Although sex of gibel carp is determined by genetic factors, it is also affected by rearing temperature (Li et al. 2016; Li and Gui 2018; Li et al. 2018). Therefore, very low proportion (<3.4%) of males were observed in the WT gynogenetic offspring (figs. 3*A* and 6*A* and supplementary fig. S13*A*, Supplementary Material online). Our results indicate that *Cg*Foxl2a-B deficiency leads to ovary development arrest and complete female to male sex reversal (fig. 3). The phenomenon is different from the defects of premature ovarian failure observed in zebrafish *foxl2a*$^{-/-}$ females (Yang et al. 2017). Along with sex reversal, the testis differentiation-related or androgen-producing genes remarkably increased their expression, but female-biased genes sharply decreased in *Cgfoxl2a-B*$^{\Delta 55/\Delta 54/\Delta 25+8}$ testis (fig. 5),

which was consistent with previous studies (Yang et al. 2017; Zhang et al. 2017; Bertho et al. 2018).

In blepharophimosis-ptosis-epicanthus inversus syndrome patients, more than 200 different *FOXL2* mutations have been found, which resulted in pleiotropic effects and clinical heterogeneity (Caburet et al. 2012; Verdin and De Baere 2012; Takahashi et al. 2013). In addition, the loss-of-function of one allele lead to *FOXL2* haploinsufficiency (Prueitt and Zinn 2001), which emphasize critical role of its correct gene dosage for normal development. Due to the varied mutations in three *Cgfoxl2a-B* alleles, we also observed the pleiotropy and haploinsufficiency effects of gonad development in this study. When in-frame mutations were produced in all *Cgfoxl2a-B* alleles and resulted in truncated *Cg*Foxl2a-B1/B2/B3 protein-lacking FKH domain, the *Cgfoxl2a-B*$^{-/-/-}$ individuals arrested ovary development at primary oocyte growth stage or developed to males. We also detected two mutated genotypes possessing WT *Cgfoxl2a-B1* allele and mutated *Cgfoxl2a-B2* and *Cgfoxl2a-B3* alleles. However, the WT *Cg*Foxl2a-B1 protein is not sufficient to keep normal ovarian development, which might be due to very low expression level of *Cgfoxl2a-B1* allele in ovary at 45 dph (fig. 2C). Interestingly, about half of *Cgfoxl2a-B* mutated individuals, which were predicted to possess two truncated *Cg*Foxl2a-B proteins without FKH domain and one mutated *Cg*Foxl2a-B protein containing an intact FKH domain, developed to normal females (fig. 3). Subcellular localization showed that the mutated *Cg*Foxl2a-B proteins with an intact FKH domain, such as *Cgfoxl2a-B2*$^{\Delta 54}$, keep transactivation capacity (fig. 5B). Importantly, *Cgfoxl2a-B2*$^{\Delta 54}$ can enhance SF1-activated *Cgcyp19a1a-A* expression (fig. 5C) similar to the previous study in Tilapia (Wang et al. 2007). We also found higher expression of mutated *Cgfoxl2a-B* alleles in ovary than that in testis at oogonia or SPG proliferation stage, which may lead to upregulated *Cgcyp19a1*as expression and downregulated *Cgdmrt1s* expression in ovary (fig. 5A). It is commonly considered that *cyp19a1a* upregulation is essential for triggering fish ovarian differentiation and its downregulation will lead to testicular differentiation (Guiguen et al. 2010). Recently, Wu et al. found that *cyp19a1a* drive ovarian differentiation by suppressing *dmrt1* (Wu et al. 2020). Therefore, this is probably the reason why about half of these mutated individuals were females, whereas the other half developed to males. Even though the regulative mechanism of *Cgfoxl2a-B2*$^{\Delta 54}$ differential expression in gibel carp early gonad development is not clear as of now, our results indicate that correct gene dosage of Foxl2a-B is critical for gibel carp ovary development.

Consistent with abundant *Cg*Foxl2b proteins distributed in oogonia and PO, complete disruption of *Cgfoxl2b-A* and *Cgfoxl2b-B* resulted in the depletion of germ cell in gibel carp (figs. 6 and 7 and supplementary table S3, Supplementary Material online). This defect was not observed in the other *foxl2* disrupted animals, implying more important roles or other function of *foxl2b* in gibel carp early oogenesis although we could not exclude the indirect function of *foxl2b* expressed in somatic cells. The dynamic expression changes of analyzed genes in germ cell depleted gonad were similar to those in testis, but opposite to those in ovary (fig. 8). The results implied that the germ cell-depleted gonad developed testis-like gonads without spermatogenic cells, consistent with our previous study in which germ cells was depleted by *dnd* morpholino-mediated knockdown approach (Liu et al. 2015). However, the compensatory increase of *Cgfoxl2a-Bs* transcripts could not rescue the defect of germ cell depletion (fig. 8). Taken together, the detailed cellular localization and function differences indicate that *Cgfoxl2a* and *Cgfoxl2b* synergize but differentially govern gibel carp folliculogenesis and gonad differentiation. As shown in figure 9B, *Cg*Foxl2a is expressed in follicular cells and complete disruption of *Cgfoxl2a* alleles leads to the upregulated expression of testis differentiation-related and androgen-producing genes, which thereby triggers testis development. *Cgfoxl2b* evolves a new function in oogenesis. In addition to expression in follicular cells, *Cg*Foxl2b is also localized in oogonia and PO, and complete deficiency of *Cgfoxl2b-A* and *Cgfoxl2b-B* alleles results in depletion of germ cells.

In total, we performed an extensive and detailed study on the origin and evolution of three *foxl2* homeologs and their alleles in the auto-allo-hexaploid gibel carp. We revealed their functional divergence by editing multiple *foxl2* homeologs and/or alleles by using CRISPR/Cas9. In conclusion, the current study covers almost all ranges of complex evolutionary scenarios associated with duplicated genes, including homeolog/allele diversification, retention/loss, biased expression, and sub-/neofunctionalization. Although theoretical presumption of these scenarios and their disparate cases have already been reported, our work has elaborated the evolutionary mechanisms involved in the duplicated *foxl2* gene.

Materials and Methods

Maintenance of Fish

Gibel carp clone F was raised and collected from the National Aquatic Biological Resource Center, NABRC. Artificial fertilization, larval hatching, and fry nursing were performed as previously described (Zhu et al. 2018). In order to eliminate the influence of environmental factors on sex, each group consisting of 100–150 WT and 100–150 *foxl2* mutated gible carp was reared in the same cage. All sampled fish were anesthetized with MS-222 (Sigma, USA). All procedures were performed with the approval of the Animal Care and Use Committee of the Institute of Hydrobiology, Chinese Academy of Sciences.

Cloning and Sequence Analysis

According to the genome sequences of gibel carp clone F (CI01000363_00413629_00414546 and ENSONIP00000026093-D2), *foxl2*a and *foxl2b* cDNAs were amplified from gibel carp ovary cDNA library by 3′ and 5′ rapid amplification of cDNA ends (supplementary table S1, Supplementary Material online). The complete cDNA sequences of 12 *foxl2* transcripts were deposited in GenBank (accession numbers from MT468195 to MT468206). Multiple amino acid sequence alignment and phylogenetic analysis were performed with DNAMAN version 7.0 and Molecular Evolutionary Genetics Analysis (MEGA 7) (Kumar et al. 2016). All the amino acid sequences used in this

study were obtained from GenBank (http://www.ncbi.nlm.nih.gov/, last accessed January 23, 2021). The accession numbers are as following: *Homo sapiens* FOXL2, NP_075555; *Mus musculus* FOXL2, NP_036150; *Gallus gallus* FOXL2, NP_001012630; *Lepisosteus oculatus* Foxl2, XP_006637658; *Latimeria chalumnae* Foxl2, XP_006001344; *Oncorhynchus mykiss* Foxl2b1, NP_001117957; *Oncorhynchus mykiss* Foxl2b2, XP_021437171; *Oreochromis niloticus* Foxl2, NP_001266707; *Ictalurus punctatus* Foxl2a, XP_017350481; *Ictalurus punctatus* Foxl2b, XP_017351917; *D. rerio* Foxl2a, NP_001038717; *D. rerio* Foxl2b, NP_001304690; *Carassius auratus* Fxol2a-B1, MT468189; *Carassius auratus* Fxol2a-B2, MT468190; *Carassius auratus* Fxol2b-A1, MT468191; *Carassius auratus* Fxol2b-A2, MT468192; *Carassius auratus* Fxol2b-B1, MT468193; and *Carassius auratus* Fxol2b-B2, MT468194. The exon–intron structure was determined by the aligning mRNA and genomic sequences of gibel carp *foxl2s*. Syntenic analyses were conducted by comparing the chromosomic regions around *foxl2s* genes in gibel carp chromosomes (*Cg*A2, *Cg*A15, and *Cg*B15) and crucian carp (*C. auratus*) chromosomes (*Ca*A2, *Ca*A15, and *Ca*B15) with corresponding regions in *H. sapiens* chromosome 3, *M. musculus* chromosome 9, *G. gallus* chromosome 9, *Xenopus tropicalis* chromosome 5, and *D. rerio* chromosomes 2 and 15. The latter information was obtained from the Ensembl (http://www.ensembl.org, last accessed January 23, 2021).

Chromosome Preparation and FISH

Chromosome preparations and FISH analyses were performed as described previously (Li, Zhang, et al. 2014). *Cgfoxl2a-B*-BAC-DNA and *Cgfoxl2b-A*-BAC-DNA labeled by DIG-Nick Translation Mix (Roche), and *Cgfoxl2b-B*-BAC-DNA labeled by Biotin-Nick Translation Mix (Roche) were used as probes.

Generation of *foxl2a-* and *foxl2b*-Mutated Gibel Carp by CRISPR/Cas9

Genome edits of gible carp *Cgfoxl2a-B*, *Cgfoxl2b-A*/*Cgfoxl2b-B*, and *Cgfoxl2a-B*/*Cgfoxl2b-A*/*Cgfoxl2b-B* by CRISPR/Cas9 were performed as described (He et al. 2018). The sgRNA target site was designed on the second exon to disrupt the FKH domain with the online service website (http://zifit.partners.org/ZiFiT/CSquare9Nuclease.aspx, last accessed January 23, 2021), and gRNA was transcribed with the TranscriptAid T7 High-Yield Transcription Kit (Thermo Fisher Scientific). The plasmid pCS2-Cas9 was digested with XbaI (NEB) and then was transcribed using the T7 mMessage mMachine Kit (Ambion) (Liu et al. 2014). About 400 pg of *Cgfoxl2a-B* sgRNA and 600 pg of Cas9 mRNA were coinjected to the one-cell stage gibel carp embryos. All of F0 individuals of *Cgfoxl2a-B* mutants grew to fertile females, of which two individuals were chosen to proliferate by gynogenesis to construct *Cgfoxl2a-B* mutant lines. Similarly, the F0 individuals with mutated *Cgfoxl2b-A*/*Cgfoxl2b-B* or mutated *Cgfoxl2a-B*/*Cgfoxl2b-A*/*Cgfoxl2b-B* were produced by simultaneously disrupted *Cgfoxl2b-A* and *Cgfoxl2b-B*, or *Cgfoxl2a-B*, *Cgfoxl2b-A*, and *Cgfoxl2b-B*. No fertile female was obtained from these two mutants.

Quantitative Reverse Transcription PCR

Tissues, including heart, liver, spleen, kidney, pituitary, hypothalamus, other brains, ovary, and testis, were sampled from 5-month gibel carp females and males. Unfertilized eggs, 50% epiboly, hatching fry, gonads from WT, and *foxl2* mutants at different stages from 10 dph to 1 year old were randomly sampled. qPCR was performed as described (Yang et al. 2017), and specific primes for each gene were listed in supplementary table S1, Supplementary Material online. Eukaryotic translation elongation factor 1 alpha 1, like 1 (*eef1a1l1*) was selected as the optimal reference gene according to our previous study (Mou et al. 2018). The relative gene expression levels were calculated with $2^{-\Delta\Delta CT}$ method (Livak and Schmittgen 2001). All the samples were analyzed in triplicates. For statistical analysis, Tukey's test was calculated with SPSS software (SPSS Inc.). A probability (P) of <0.05 was considered statistically significant.

In order to analyze the expression difference among three alleles of each *foxl2* genes, the qPCR products amplified from ovary (45 and 270 dph) and testis (45 and 150 dph) ($n = 3$) were purified and cloned into Trans5α Chemically Competent Cell. About 20–30 clones of each sample were sequenced and classified according to the specific SNPs in three alleles. The average ratios of sequencing clone numbers were used to show the expression levels.

Polyclonal Antibody Preparation, Western Blot, Histological Section, and Immunofluorescence

Polyclonal antibodies, respectively, specific to the *Cg*Foxl2a and *Cg*Foxl2b were produced by Friendbio Science and Technology (Wuhan) Co. Ltd. Western blot, histological section, and immunofluorescence were performed as described previously (Liu et al. 2015; Yang et al. 2017), and the results were acquired with ImageQuant LAS 4000mini (GE) and Carl Zeiss upright fluorescence microscope Axio Imager M2 (Analytical and Testing Center, IHB, CAS), respectively.

Subcellular Localization

WT *Cgfoxl2a-B2*, *Cgfoxl2a-B2*$^{\Delta 54}$, *Cgfoxl2a-B1*$^{\Delta 55}$, and *Cgfoxl2a-B3*$^{\Delta 25+8}$ were subcloned into *Xho*I/*Kpn*I sites of pEGFP-N3 vector (BD Biosciences Clontech). All the plasmids were verified by sequence analysis. One microgram plasmids were transfected into HEK293T cells. The cell culture, transfection, fixation, and nuclear staining with 4′, 6-diamidino-2-phenylindole (DAPI) were performed as previously described (Lu et al. 2018). The results were acquired by Carl Zeiss upright fluorescence microscope Axio imager M2 (Analytical and Testing Center, IHB, CAS).

Plasmid Constructs

For luciferase assays, expression plasmids were generated by cloning the full length ORF of WT *Cgfoxl2a-B2*, *Cgfoxl2a-B2*$^{\Delta 54}$, *Cgfoxl2a-B1*$^{\Delta 55}$, and *Cgfoxl2a-B3*$^{\Delta 25+8}$ were subcloned into *Kpn*I/*Xho*I sites of pcDNA3.1(+) vector. *Cgsf1a-B* was subcloned into *Nhe*I/*Hin*dIII sites of pcDNA3.1(+) vector. For promoter activity analysis, 1,329 and 1,140 bp 5′-flanking regulatory region of *Cgcyp19a1a-A* promoter (GenBank accession number MW160449) and *Cgcyp19a1a-B* promoter

(GenBank accession number MW160450) were subcloned into *Kpn*I/*Xho*I sites of pGL3-basic luciferase reporter vector (*Cgcyp19a1a-A*pro-luc and *Cgcyp19a1a-B*pro-luc), respectively. All constructs were verified by sequencing.

Transfection and Luciferase Activity Assays

CAB and EPC were seeded overnight in 24-well plates and transfected using FuGENE HD Transfection Reagent (Promega) with various plasmids at a ratio of 10:10:1 (200 ng expression plasmid: 200 ng *Cgcyp19a1a-A* pro-luc or *Cgcyp19a1a-B* pro-luc plasmid: 20 ng Renilla luciferase plasmid pRL-TK). Empty vector (pcDNA3.1) was adjusted to ensure DNA concentration in total among wells. Transient transfections and luciferase activity assays were performed as described (Lu, Zhou, et al. 2020). Luciferase activities were measured by a Junior LB9509 luminometer (Berthold, Pforzheim, Germany) and normalized to that of Renilla luciferase activity. All experiments were performed in triplicate and the significant differences were calculated by SPSS software (SPSS Inc.).

Supplementary Material

Supplementary data are available at *Molecular Biology and Evolution* online.

Acknowledgments

We thank the anonymous reviewers for helpful discussion in editing this manuscript. This work was supported by the National Key Research and Development Program of China (Grant No. 2018YFD0900204), the Key Program of Frontier Sciences of the Chinese Academy of Sciences (Grant No. QYZDY-SSW-SMC025), and China Agriculture Research System (Grant No. CARS-45-07).

Author Contributions

J.-F.G., L.Z., R.-H.G. designed the study. R.-H.G., Z.L., Z.-X.Y., X.-Y.L., J.-F.T., and X.-J.Z. prepared the samples and carried out the experiments. R.-H.G., L.Z., J.-F.G., and Y.W. analyzed and discussed the results. L.Z., J.-F.G., Y.W., and R.-H.G. wrote the paper.

Data Availability

The DNA sequences have been deposited at National Center for Biotechnology Information (NCBI), accession numbers MW160449, MW160450, and MT468189–MT468206. All other data are available from the corresponding authors upon reasonable request.

References

Alam MA, Kobayashi Y, Horiguchi R, Hirai T, Nakamura M. 2008. Molecular cloning and quantitative expression of sexually dimorphic markers Dmrt1 and Foxl2 during female-to-male sex change in *Epinephelus merra*. *Gen Comp Endocrinol*. 157(1):75–85.

Amores A, Force A, Yan YL, Joly L, Amemiya C, Fritz A, Ho RK, Langeland J, Prince V, Wang YL, et al. 1998. Zebrafish hox clusters and vertebrate genome evolution. *Science* 282(5394):1711–1714.

Berthelot C, Brunet F, Chalopin D, Juanchich A, Bernard M, Noel B, Bento P, Da SC, Labadie K, Alberti A, et al. 2014. The rainbow trout genome provides novel insights into evolution after whole-genome duplication in vertebrates. *Nat Commun*. 5(1):3657.

Bertho S, Herpin A, Branthonne A, Jouanno E, Yano A, Nicol B, Muller T, Pannetier M, Pailhoux E, Miwa M, et al. 2018. The unusual rainbow trout sex determination gene hijacked the canonical vertebrate gonadal differentiation pathway. *Proc Natl Acad Sci U S A*. 115(50):12781–12786.

Bertho S, Pasquier J, Pan Q, Le Trionnaire G, Bobe J, Postlethwait JH, Pailhoux E, Schartl M, Herpin A, Guiguen Y. 2016. Foxl2 and its relatives are evolutionary conserved players in gonadal sex differentiation. *Sex Dev*. 10(3):111–129.

Bhat IA, Rather MA, Dar JY, Sharma R. 2016. Molecular cloning, computational analysis and expression pattern of Forkhead boxl2 (Foxl2) gene in catfish. *Comput Biol Chem*. 64:9–18.

Boulanger L, Pannetier M, Gall L, Allais-Bonnet A, Elzaiat M, Le Bourhis D, Daniel N, Richard C, Cotinot C, Ghyselinck NB, et al. 2014. *FOXL2* is a female sex-determining gene in the goat. *Curr Biol*. 24(4):404–408.

Caburet S, Georges A, L'Hôte D, Todeschini A-L, Benayoun BA, Veitia RA. 2012. The transcription factor FOXL2: at the crossroads of ovarian physiology and pathology. *Mol Cell Endocrinol*. 356(1–2):55–64.

Caulier M, Brion F, Chadili E, Turies C, Piccini B, Porcher J, Guiguen Y, Hinfray N. 2015. Localization of steroidogenic enzymes and Foxl2a in the gonads of mature zebrafish (*Danio rerio*). *Comp Biochem Physiol A Mol Integr Physiol*. 188:96–106.

Cheng F, Wu J, Cai X, Liang J, Freeling M, Wang X. 2018. Gene retention, fractionation and subgenome differences in polyploid plants. *Nat Plants*. 4(5):258–268.

Clark JW, Donoghue P. 2018. Whole-genome duplication and plant macroevolution. *Trends Plant Sci*. 23(10):933–945.

Cocquet J, Pailhoux E, Jaubert F, Servel N, Xia X, Pannetier M, De Baere E, Messiaen L, Cotinot C, Fellous M. 2002. Evolution and expression of *FOXL2*. *J Med Genet*. 39(12):916–921.

Comai L. 2005. The advantages and disadvantages of being polyploid. *Nat Rev Genet*. 6(11):836–846.

Crisponi L, Deiana M, Loi A, Chiappe F, Uda M, Amati P, Bisceglia L, Zelante L, Nagaraja R, Porcu S, et al. 2001. The putative Forkhead transcription factor *FOXL2* is mutated in blepharophimosis/ptosis/epicanthus inversus syndrome. *Nat Genet*. 27(2):159–166.

Doyle JJ, Flagel LE, Paterson AH, Rapp RA, Soltis DE, Soltis PS, Wendel JF. 2008. Evolutionary genetics of genome merger and doubling in plants. *Annu Rev Genet*. 42(1):443–461.

Edger PP, Smith R, McKain MR, Cooley AM, Vallejo-Marin M, Yuan Y, Bewick AJ, Ji L, Platts AE, Bowman MJ, et al. 2017. Subgenome dominance in an interspecific hybrid, synthetic allopolyploid, and a 140-year-old naturally established neo-allopolyploid monkeyflower. *Plant Cell*. 29(9):2150–2167.

Forconi M, Canapa A, Barucca M, Biscotti MA, Capriglione T, Buonocore F, Fausto AM, Makapedua DM, Pallavicini A, Gerdol M, et al. 2013. Characterization of sex determination and sex differentiation genes in *Latimeria*. *PLoS One*. 8(4):e56006.

Govoroun MS, Pannetier M, Pailhoux E, Cocquet J, Brillard JP, Couty I, Batellier F, Cotinot C. 2004. Isolation of chicken homolog of the *FOXL2* gene and comparison of its expression patterns with those of aromatase during ovarian development. *Dev Dyn*. 231(4):859–870.

Grier H. 2000. Ovarian germinal epithelium and folliculogenesis in the common snook, *Centropomus undecimalis* (Teleostei: centropomidae). *J Morphol*. 243(3):265–281.

Grier HJ. 2012. Development of the follicle complex and oocyte staging in red drum, *Sciaenops ocellatus* Linnaeus, 1776 (Perciformes, Sciaenidae). *J Morphol*. 273(8):801–829.

Grier HJ, Uribe-Aranzábal MC, Patino R. 2009. The ovary, folliculogenesis, and oogenesis in teleosts. In: Jamieson BGM, editor. Reproductive biology and phylogeny of fishes (agnathans and bony fishes). Enfield (NH): Science Publishers. p. 25–84.

Gui JF, Zhou L. 2010. Genetic basis and breeding application of clonal diversity and dual reproduction modes in polyploid *Carassius auratus gibelio*. *Sci China Life Sci*. 53(4):409–415.

Guiguen Y, Fostier A, Piferrer F, Chang CF. 2010. Ovarian aromatase and estrogens: a pivotal role for gonadal sex differentiation and sex change in fish. *Gen Comp Endocrinol*. 165(3):352–366.

He WX, Wu M, Liu Z, Li Z, Wang Y, Zhou J, Yu P, Zhang XJ, Zhou L, Gui JF. 2018. Oocyte-specific maternal Slbp2 is required for replication-dependent histone storage and early nuclear cleavage in zebrafish oogenesis and embryogenesis. *RNA*. 24(12):1738–1748.

Herpin A, Adolfi MC, Nicol B, Hinzmann M, Schmidt C, Klughammer J, Engel M, Tanaka M, Guiguen Y, Schartl M. 2013. Divergent expression regulation of gonad development genes in medaka shows incomplete conservation of the downstream regulatory network of vertebrate sex determination. *Mol Biol Evol*. 30(10):2328–2346.

Ijiri S, Kaneko H, Kobayashi T, Wang DS, Sakai F, Paul-Prasanth B, Nakamura M, Nagahama Y. 2008. Sexual dimorphic expression of genes in gonads during early differentiation of a teleost fish, the Nile tilapia *Oreochromis niloticus*. *Biol Reprod*. 78(2):333–341.

Iwade R, Maruo K, Okada G, Nakamura M. 2008. Elevated expression of *P450c17* (*CYP17*) during testicular formation in the frog. *Gen Comp Endocrinol*. 155(1):79–87.

Jagarlamudi K, Rajkovic A. 2012. Oogenesis: transcriptional regulators and mouse models. *Mol Cell Endocrinol*. 356(1–2):31–39.

Jiang FF, Wang ZW, Zhou L, Jiang L, Zhang XJ, Apalikova OV, Brykov VA, Gui JF. 2013. High male incidence and evolutionary implications of triploid form in northeast Asia *Carassius auratus* complex. *Mol Phylogenet Evol*. 66(1):350–359.

Jiang SY, Wang Y, Zhou L, Chen F, Li Z, Gui JF. 2020. Molecular characteristics, genomic structure and expression patterns of diverse *bmp15* alleles in polyploid gibel carp clone F. *Acta Hydrobiol Sin*. 44:518–527.

Kayampilly PP, Wanamaker BL, Stewart JA, Wagner CL, Menon KM. 2010. Stimulatory effect of insulin on 5alpha-reductase type 1 (SRD5A1) expression through an Akt-dependent pathway in ovarian granulosa cells. *Endocrinology* 151(10):5030–5037.

Kocer A, Pinheiro I, Pannetier M, Renault L, Parma P, Radi O, Kim KA, Camerino G, Pailhoux E. 2008. *R-spondin1* and *FOXL2* act into two distinct cellular types during goat ovarian differentiation. *BMC Dev Biol*. 8(1):36.

Kumar S, Stecher G, Tamura K. 2016. MEGA7: molecular evolutionary genetics analysis version 7.0 for bigger datasets. *Mol Biol Evol*. 33(7):1870–1874.

Leggatt RA, Iwama GK. 2003. Occurrence of polyploidy in the fishes. *Rev Fish Biol Fisher*. 13(3):237–246.

Li XY, Gui JF. 2018. Diverse and variable sex determination mechanisms in vertebrates. *Sci China Life Sci*. 61(12):1503–1514.

Li XY, Li Z, Zhang XJ, Zhou L, Gui JF. 2014. Expression characterization of testicular DMRT1 in both Sertoli cells and spermatogenic cells of polyploid gibel carp. *Gene* 548(1):119–125.

Li XY, Liu XL, Ding M, Li Z, Zhou L, Zhang XJ, Gui JF. 2017. A novel male-specific SET domain-containing gene *Setdm* identified from extra microchromosomes of gibel carp males. *Sci Bull*. 62(8):528–536.

Li XY, Liu XL, Zhu YJ, Zhang J, Ding M, Wang MT, Wang ZW, Li Z, Zhang XJ, Zhou L, et al. 2018. Origin and transition of sex determination mechanisms in a gynogenetic hexaploid fish. *Heredity (Edinburgh)* 121(1):64–74.

Li XY, Zhang QY, Zhang J, Zhou L, Li Z, Zhang XJ, Wang D, Gui JF. 2016. Extra microchromosomes play male determination role in polyploid gibel carp. *Genetics* 203(3):1415–1424.

Li XY, Zhang XJ, Li Z, Hong W, Liu W, Zhang J, Gui JF. 2014. Evolutionary history of two divergent *Dmrt1* genes reveals two rounds of polyploidy origins in gibel carp. *Mol Phylogenet Evol*. 78:96–104.

Lien S, Koop BF, Sandve SR, Miller JR, Kent MP, Nome T, Hvidsten TR, Leong JS, Minkley DR, Zimin A, et al. 2016. The Atlantic salmon genome provides insights into rediploidization. *Nature* 533(7602):200–205.

Liu D, Wang Z, Xiao A, Zhang Y, Li W, Zu Y, Yao S, Lin S, Zhang B. 2014. Efficient gene targeting in zebrafish mediated by a zebrafish-codon-optimized cas9 and evaluation of off-targeting effect. *J Genet Genom*. 41(1):43–46.

Liu S, Li Z, Gui JF. 2009. Fish-specific duplicated *dmrt2b* contributes to a divergent function through Hedgehog pathway and maintains left-right asymmetry establishment function. *PLoS One*. 4(9):e7261.

Liu W, Li SZ, Li Z, Wang Y, Li XY, Zhong JX, Zhang XJ, Zhang J, Zhou L, Gui JF. 2015. Complete depletion of primordial germ cells in an All-female fish leads to Sex-biased gene expression alteration and sterile All-male occurrence. *BMC Genomics* 16(1):971.

Liu XL, Jiang FF, Wang ZW, Li XY, Li Z, Zhang XJ, Chen F, Mao JF, Zhou L, Gui JF. 2017. Wider geographic distribution and higher diversity of hexaploids than tetraploids in *Carassius* species complex reveal recurrent polyploidy effects on adaptive evolution. *Sci Rep*. 7(1):5395.

Liu XL, Li XY, Jiang FF, Wang ZW, Li Z, Zhang XJ, Zhou L, Gui JF. 2017. Numerous mitochondrial DNA haplotypes reveal multiple independent polyploidy origins of hexaploids in *Carassius* species complex. *Ecol Evol*. 7(24):10604–10615.

Liu Z, Chen A, Yang Z, Wei H, Leng X. 2012. Molecular characterization of growth differentiation factor 9 and its spatio-temporal expression pattern in gibel carp (*Carassius auratus gibelio*). *Mol Biol Rep*. 39(4):3863–3870.

Livak KJ, Schmittgen TD. 2001. Analysis of relative gene expression data using real-time quantitative PCR and the 2(-Delta Delta C(T)) method. *Methods* 25(4):402–408.

Loffler KA, Zarkower D, Koopman P. 2003. Etiology of ovarian failure in blepharophimosis ptosis epicanthus inversus syndrome: *FOXL2* is a conserved, early-acting gene in vertebrate ovarian development. *Endocrinology* 144(7):3237–3243.

Lu M, Li XY, Li Z, Du WX, Zhou L, Wang Y, Zhang XJ, Wang ZW, Gui JF. 2021. Regain of sex determination system and sexual reproduction ability in a synthetic octoploid male fish. *Sci China Life Sci*. 64(1):77–87.

Lu WJ, Zhou L, Gao FX, Sun ZH, Li Z, Liu XC, Li SS, Wang Y, Gui JF. 2018. Divergent expression patterns and function of two *cxcr4* paralogs in hermaphroditic *Epinephelus coioides*. *IJMS* 19(10):2943.

Lu WJ, Zhou L, Gao FX, Zhou YL, Li Z, Zhang XJ, Wang Y, Gui JF. 2020. Dynamic and differential expression of duplicated Cxcr4/Cxcl12 genes facilitates antiviral response in hexaploid gibel carp. *Front Immunol*. 11:2176.

Luo J, Chai J, Wen Y, Tao M, Lin G, Liu X, Ren L, Chen Z, Wu S, Li S, et al. 2020. From asymmetrical to balanced genomic diversification during rediploidization: subgenomic evolution in allotetraploid fish. *Sci Adv*. 6(22):eaaz7677.

Mandakova T, Lysak MA. 2018. Post-polyploid diploidization and diversification through dysploid changes. *Curr Opin Plant Biol*. 42:55–65.

McClintock B. 1984. The significance of responses of the genome to challenge. *Science* 226(4676):792–801.

Meyer A, Van de Peer Y. 2005. From 2R to 3R: evidence for a fish-specific genome duplication (FSGD). *Bioessays* 27(9):937–945.

Mou CY, Wang Y, Zhang QY, Gao FX, Li Z, Tong JF, Zhou L, Gui JF. 2018. Differential interferon system gene expression profiles in susceptible and resistant gynogenetic clones of gibel carp challenged with herpesvirus CaHV. *Dev Comp Immunol*. 86:52–64.

Nakamoto M, Matsuda M, Wang DS, Nagahama Y, Shibata N. 2006. Molecular cloning and analysis of gonadal expression of *Foxl2* in the medaka, *Oryzias latipes*. *Biochem Biophys Res Commun*. 344(1):353–361.

Neaves WB, Baumann P. 2011. Unisexual reproduction among vertebrates. *Trends Genet*. 27(3):81–88.

Ng DW, Lu J, Chen ZJ. 2012. Big roles for small RNAs in polyploidy, hybrid vigor, and hybrid incompatibility. *Curr Opin Plant Biol*. 15(2):154–161.

Otto SP. 2007. The evolutionary consequences of polyploidy. *Cell* 131(3):452–462.

Park SY, Jameson JL. 2005. Minireview: transcriptional regulation of gonadal development and differentiation. *Endocrinology* 146(3):1035–1042.

Payne AH, Hales DB. 2004. Overview of steroidogenic enzymes in the pathway from cholesterol to active steroid hormones. *Endocr Rev*. 25(6):947–970.

Pisarska MD, Bae J, Klein C, Hsueh AJ. 2004. Forkhead l2 is expressed in the ovary and represses the promoter activity of the steroidogenic acute regulatory gene. *Endocrinology* 145(7):3424–3433.

Prueitt RL, Zinn AR. 2001. A fork in the road to fertility. *Nat Genet*. 27(2):132–134.

Quagio-Grassiotto I, Grier H, Mazzoni TS, Nobrega RH, de Arruda AJ. 2011. Activity of the ovarian germinal epithelium in the freshwater catfish, *Pimelodus maculatus* (Teleostei: Ostariophysi: Siluriformes): germline cysts, follicle formation and oocyte development. *J Morphol*. 272(11):1290–1306.

Ramirez-Gonzalez RH, Borrill P, Lang D, Harrington SA, Brinton J, Venturini L, Davey M, Jacobs J, van Ex F, Pasha A, et al. 2018. The transcriptional landscape of polyploid wheat. *Science* 361(6403):eaar6089.

Richards JS, Ren YA, Candelaria N, Adams JE, Rajkovic A. 2018. Ovarian follicular theca cell recruitment, differentiation, and impact on fertility: 2017 update. *Endocr Rev*. 39(1):1–20.

Schmidt D, Ovitt CE, Anlag K, Fehsenfeld S, Gredsted L, Treier AC, Treier M. 2004. The murine winged-helix transcription factor Foxl2 is required for granulosa cell differentiation and ovary maintenance. *Development* 131(4):933–942.

Sessa EB. 2019. Polyploidy as a mechanism for surviving global change. *New Phytol*. 221(1):5–6.

Soltis PS, Liu X, Marchant DB, Visger CJ, Soltis DE. 2014. Polyploidy and novelty: gottlieb's legacy. *Philos Trans R Soc B*. 369(1648):20130351.

Soltis PS, Soltis DE. 2016. Ancient WGD events as drivers of key innovations in angiosperms. *Curr Opin Plant Biol*. 30:159–165.

Song Q, Chen ZJ. 2015. Epigenetic and developmental regulation in plant polyploids. *Curr Opin Plant Biol*. 24:101–109.

Takahashi A, Kimura F, Yamanaka A, Takebayashi A, Kita N, Takahashi K, Murakami T. 2013. The *FOXL2* mutation (c.402C>G) in adult-type ovarian granulosa cell tumors of three Japanese patients: clinical report and review of the literature. *Tohoku J Exp Med*. 231:243–250.

Taylor JS. 2003. Genome duplication, a trait shared by 22,000 species of ray-finned fish. *Genome Res*. 13(3):382–390.

Uhlenhaut NH, Jakob S, Anlag K, Eisenberger T, Sekido R, Kress J, Treier AC, Klugmann C, Klasen C, Holter NI, et al. 2009. Somatic sex reprogramming of adult ovaries to testes by FOXL2 ablation. *Cell* 139(6):1130–1142.

Van de Peer Y, Maere S, Meyer A. 2009. The evolutionary significance of ancient genome duplications. *Nat Rev Genet*. 10(10):725–732.

Van de Peer Y, Mizrachi E, Marchal K. 2017. The evolutionary significance of polyploidy. *Nat Rev Genet*. 18(7):411–424.

Van de Peer Y, Taylor JS, Meyer A. 2003. Are all fishes ancient polyploids? *J Struct Funct Genomics*. 3(1–4):65–73.

Verdin H, De Baere E. 2012. *FOXL2* impairment in human disease. *Horm Res Paediatr*. 77(1):2–11.

Vizziano D, Randuineau G, Baron D, Cauty C, Guiguen Y. 2007. Characterization of early molecular sex differentiation in rainbow trout, *Oncorhynchus mykiss*. *Dev Dyn*. 236(8):2198–2206.

Wang DS, Kobayashi T, Zhou LY, Paul-Prasanth B, Ijiri S, Sakai F, Okubo K, Morohashi K, Nagahama Y. 2007. Foxl2 up-regulates aromatase gene transcription in a female-specific manner by binding to the promoter as well as interacting with ad4 binding protein/steroidogenic factor 1. *Mol Endocrinol*. 21(3):712–725.

Wu K, Song W, Zhang Z, Ge W. 2020. Disruption of *dmrt1* rescues the all-male phenotype of the *cyp19a1a* mutant in zebrafish - a novel insight into the roles of aromatase/estrogens in gonadal differentiation and early folliculogenesis. *Development* 147(4):dev182758.

Wu TD, Watanabe CK. 2005. GMAP: a genomic mapping and alignment program for mRNA and EST sequences. *Bioinformatics* 21(9):1859–1875.

Xiong Z, Gaeta RT, Pires JC. 2011. Homoeologous shuffling and chromosome compensation maintain genome balance in resynthesized allopolyploid *Brassica napus*. *Proc Natl Acad Sci U S A*. 108(19):7908–7913.

Xu H, Gui J, Hong Y. 2005. Differential expression of *vasa* RNA and protein during spermatogenesis and oogenesis in the gibel carp (*Carassius auratus gibelio*), a bisexually and gynogenetically reproducing vertebrate. *Dev Dyn*. 233(3):872–882.

Xu P, Zhang X, Wang X, Li J, Liu G, Kuang Y, Xu J, Zheng X, Ren L, Wang G, et al. 2014. Genome sequence and genetic diversity of the common carp, *Cyprinus carpio*. *Nat Genet*. 46(11):1212–1219.

Yang J, Liu D, Wang X, Ji C, Cheng F, Liu B, Hu Z, Chen S, Pental D, Ju Y, et al. 2016. The genome sequence of allopolyploid *Brassica juncea* and analysis of differential homoeolog gene expression influencing selection. *Nat Genet*. 48(10):1225–1232.,

Yang YJ, Wang Y, Li Z, Zhou L, Gui JF. 2017. Sequential, divergent, and cooperative requirements of *foxl2a* and *foxl2b* in ovary development and maintenance of zebrafish. *Genetics* 205(4):1551–1572.

Yu P, Wang Y, Yang WT, Li Z, Zhang XJ, Zhou L, Gui JF. 2021. Upregulation of the PPAR signaling pathway and accumulation of lipids are related to the morphological and structural transformation of the dragon-eye goldfish eye. *Sci China Life Sci*. doi: 10.1007/s11427-020-1814-1.

Zhang J, Sun M, Zhou L, Li Z, Liu Z, Li XY, Liu XL, Liu W, Gui JF. 2015. Meiosis completion and various sperm responses lead to unisexual and sexual reproduction modes in one clone of polyploid *Carassius gibelio*. *Sci Rep*. 5(1):10898.

Zhang QQ, Zhou L, Li Z, Gan RH, Yu ZX, Gui JF, Wang Y. 2020. Allelic diversification, syntenic alignment and expression patterns of *nanos2* in polyploid gibel carp. *Acta Hydrobiol Sin*. 44:1087–1096.

Zhang X, Li M, Ma H, Liu X, Shi H, Li M, Wang D. 2017. Mutation of *foxl2* or *cyp19a1a* results in female to male sex reversal in XX Nile Tilapia. *Endocrinology* 158:2634–2647.

Zhou L, Gui JF. 2002. Karyotypic diversity in polyploid gibel carp, *Carassius auratus gibelio* Bloch. *Genetica* 115(2):223–232.

Zhou L, Gui JF. 2017. Natural and artificial polyploids in aquaculture. *Aquacult Fish*. 2(3):103–111.

Zhu HP, Ma DM, Gui JF. 2006. Triploid origin of the gibel carp as revealed by 5S rDNA localization and chromosome painting. *Chromosome Res*. 14(7):767–776.

Zhu YJ, Li XY, Zhang J, Li Z, Ding M, Zhang XJ, Zhou L, Gui JF. 2018. Distinct sperm nucleus behaviors between genotypic and temperature-dependent sex determination males are associated with replication and expression-related pathways in a gynogenetic fish. *BMC Genomics*. 19(1):437.